nature communications

Article

https://doi.org/10.1038/s41467-025-63228-1

Root-to-shoot mobile mRNA *CmoKARI1* promotes JA-Ile biosynthesis to confer chilling tolerance in grafted cucumbers

Received: 3 December 2023

Accepted: 13 August 2025

Published online: 21 August 2025

Check for updates

Miao Zhang[1,6], Wenqian Liu[1,6], Cuicui Wang[1,6], Shujin Lin[2,6], Ying Chen[1], Heran Cui[1], Chenggang Xiang[3], Yujia Ma[1], Xiaojun Li[1], Yongzhen Lu[1], Xiao Han[2], Yihan Dong[4,5], Lihong Gao[1] & Wenna Zhang[1]

Pumpkin rootstock is commonly used to graft cucurbit crops, improving their ability to withstand stress. While the significance of systemic signals from rootstocks to scions is recognized, the role of root-to-shoot transported mRNAs remains understudied. Cucumber plants often face growth and productivity limitations due to low temperatures. To shed light on the enhancement of chilling tolerance in grafted cucumber scions by pumpkin-derived mRNAs, we revisit the metabolomic and transcriptomic dataset from the cucumber/pumpkin heterograft under chilling condition. We identify pumpkin *Ketol-acid reductoisomerase 1* (*CmoKARI1*) as the key mobile mRNA that specifically travels from pumpkin rootstock to cucumber scion upon early chilling stress. Overexpressing *CmoKARI1* results in increased isoleucine level and chilling tolerance in both cucumber and Arabidopsis. The increased isoleucine is further used to synthesize JA-Ile conjugates, activating JA-Ile signaling and enabling heterografts to weather low temperatures. This study represents the instance of a unidirectional mobile mRNA triggered by specific environmental cues.

Climate change caused increasing and unpredictable chilling stress (>0 °C). To cope with low temperatures, plants have developed intricate mechanisms[1,2]. Different from chilling stress, freezing stress, characterized by temperatures below zero, can lead to the formation of ice crystals that damage membrane systems. While some crops, like winter wheat, exhibit resilience to freezing stress, others, such as cucumber (*Cucumis sativus* L.), are susceptible to being fatally impacted by chilling stress (<10 °C)[3]. Although the underlying mechanisms for these variations remain insufficiently understood, both chilling and freezing stress responses are governed by conserved genetic factors. One of the most extensively studied transcription factors is the C-repeat binding factor/dehydration-responsive element binding protein 1 (CBF/DREB1)[4]. CBF/DREB1 specifically binds to the CRT/DRE sequence present in the promoter regions of cold-responsive genes (*COR*)[5]. This regulatory interaction initiates the transcriptional activation of *COR* genes. CBF Expression 1 (ICE1), a MYC-type transcription factor, is the most-studied activator of *CBF* transcription. The stability of ICE is upheld by phosphorylated Open Stomata 1 (OST1) and MPK3, which transduce signals stemming from upstream reactive oxygen species (ROS) or calcium fluctuations induced by lowered temperatures[1].

To enhance cucumber's chilling tolerance, grafting with pumpkin rootstocks such as figleaf gourd (*Cucurbita ficifolia* Bouché) and other pumpkin varieties (e.g., *Cucurbita moschata*) has become a widely

[1]Beijing Key Laboratory of Growth and Developmental Regulation for Protected Vegetable Crops, China Agricultural University, Beijing 100193, China. [2]College of Biology Science and Engineering, Fuzhou University, Fuzhou 350116, China. [3]College of Life Science and Technology, Honghe University, Mengzi, Yunnan 661100, China. [4]Institut de Biologie Moléculaire des Plantes, Centre National de la Recherche Scientifique, UPR 2357, Université de Strasbourg, 67000 Strasbourg, France. [5]Present address: Institut de Génétique et de Biologie Moléculaire et Cellulaire, 67404 Illkirch, France. [6]These authors contributed equally: Miao Zhang, Wenqian Liu, Cuicui Wang, Shujin Lin. e-mail: zhangwenna@cau.edu.cn

adopted method during the chilling season for cultivation[6,7]. Different rootstock resources confer varying levels of chilling tolerance to the scion[7], indicating the existence of long-distance signals from rootstocks to scions. Among these long-distance signals, e.g., nutrients and ROS, many influence crucial agricultural traits such as flavor and yield[6]. Therefore, uncovering the mechanism underlying these rootstock-to-scion signals in grafted cucumbers under chilling conditions holds significant importance. A recent study uncovered accumulation of jasmonates (JAs) in the scions to be crucial for chilling tolerance in heterografts of tomatoes and watermelons[8–10]. JAs play crucial roles as phytohormones in promoting chilling tolerance in plants[11]. Chilling triggers a rapid increase in JA biosynthesis and activates JA signaling pathways. Application of JAs has been shown to enhance chilling tolerance in tomatoes and apples by positively regulating the ICE1-CBF pathway[10,12,13]. Particularly in cucumber, JA triggers degradation of JAZ5, thereby allowing direct ICE1 binding to the promoter of *CsCBF1*[14]. In *planta*, JA-Ile, the most abundant active form of JA, is synthesized through the conjugation of JA with isoleucine, a reaction catalyzed by Jasmonic acid-amido synthetase 1 (JAR1). The highly induced endogenous JA-Ile is perceived by the JA receptor Coronatine Insensitive 1 (COI1), which interacts with Jasmonate Zim Domain proteins (JAZs), leading to their ubiquitination and subsequent degradation via the 26S proteasome pathway[15–18]. This process activates downstream transcription factors and confers resistance to biotic and abiotic stresses in plants[11]. However, the mechanism by which the rootstock leads to elevated levels of JAs in the grafted scions remains a subject of debate. Given that JAs cannot move from root to shoot[19], other components involved in JA biosynthesis are likely delivered from the pumpkin rootstock upon chilling stress.

Increasing evidence highlights the critical role of mobile mRNAs as systemic signaling molecules between rootstock and scions[20,21], exemplified by various transcripts such as *CmNACP*[22], *KNOTTED1*[23], *StBEL5*[24], *PFP-LET6*[25], *CmGAIP*[26], *PEBP*[27], *AtTCTP1*[28], *SlPS*[29], *HSP70*[28,30], *PbWoxT1*[31,32], and *PbDRM*[33]. These mobile mRNAs, akin to small RNAs[28,34], are predominantly transported from shoot to root via the phloem stream along with photosynthates[28,35], which can hardly explain the function of pumpkin as rootstocks. The specific role of mobile mRNAs in the exchange between pumpkin rootstocks and cucumber scions has been characterized on a large scale, revealing an association of mobile mRNAs with fatty acid and amino acid metabolism under chilling stress[36]. Nonetheless, the precise mechanisms by which fatty acid and amino acid metabolism contribute to chilling tolerance, as well as the potential key mRNAs provided by pumpkin rootstocks to enhance chilling tolerance in cucumber scions, are yet to be elucidated.

In this study, we identified a specific mRNA *CmoKARI1*, which plays a crucial role in enhancing chilling stress tolerance in cucumber (Csa)/pumpkin (Cmo) heterografts. Interestingly, we found that pumpkin rootstock selectively transports *KARI1* to the cucumber scion in response to chilling stress, while cucumber is unable to transport its own *KARI1* upwards to the shoot. Through the overexpression of *CmoKARI1* in both cucumber and Arabidopsis, we unraveled the significance of this gene in conferring chilling tolerance. Notably, *KARI1* encodes an enzyme involved in the synthesis of branched-chain amino acids (BCAAs). Of the exogenously applied BCAAs, only isoleucine (Ile) was effective in enhancing chilling tolerance in cucumber. This led us to investigate the JA-Ile pathway. As a result of *CmoKARI1* overexpression, we observed a significant increase in both Ile and JA-Ile levels upon chilling stress, subsequently activating the JA-Ile signaling pathway. Furthermore, inhibition of JA-Ile synthesis compromised chilling tolerance in *CmoKARI1* overexpression lines. Our findings present the pioneering case of a root-to-shoot mobile mRNA triggered by specific environmental stimuli, offering valuable insights for future advancements in crop breeding and grafting techniques.

Results

Integrated analysis of transcript and metabolite profiles reveals an important role of *CmoKARI1* in cucumber heterografts upon chilling stress

Pumpkin rootstock is widely employed to enhance stress tolerance in heterografts. To shed light on the essential mobile RNA signals transmitted from pumpkin (Cmo) rootstocks to cucumber (Csa) scions during chilling stress, we re-examined previously identified mobile transcript data from Cmo rootstock and Csa scion samples of reciprocally grafted seedlings subjected to chilling stress[36,37]. Venn analysis revealed that 3460 Csa transcripts and 99 Cmo transcripts were transported upon chilling stress (Supplementary Fig. 1a; Supplementary Dataset 1). Remarkably, among the 99 chilling-induced mobile Cmo transcripts, 80 transcripts were exclusively transported from Cmo rootstocks to Csa scions (Fig. 1a; Supplementary Fig. 1b, c). KEGG enrichment analysis highlighted that these 80 transcripts were enriched in pathways related to the biosynthesis of branched-chain amino acids as well as other metabolic pathways ($p = 0.092$) (Fig. 1b; Supplementary Dataset 2).

To assess the metabolic consequences of the 80 mobile mRNAs, we examined the metabolomic data obtained from the same Csa tissues of heterografts[36]. We identified 175 differentially induced metabolites (CsaDIMs) between Csa/Csa homograft and Csa/Cmo heterograft in response to chilling stress. 11 CsaDIMs were enriched in the BCAA biosynthesis pathway (ko00290) ($p = 0.0000911$) (Fig. 1c; Supplementary Fig. 2a, b; Supplementary Dataset 3 and 4). Notably, L-Isoleucine, L-Leucine, and (R)−2-Methylmalate exhibited substantial accumulation in the leaves of cucumber in Csa/Cmo heterografts under chilling conditions (Fig. 1d; Supplementary Fig. 2c).

To explore the relationships between BCAA-related CsaDIMs and cold-induced CsaDEGs, a correlation analysis was conducted. Remarkably, the 11 BCAA-related CsaDIMs in Csa leaves of Csa/Cmo grafts showed significant correlations with 361 cold-induced CsaDEGs (Person $|cor| \geq 0.95$, p-value < 0.05) (Supplementary Data 5; Supplementary Data 6). Utilizing Cytoscape based on the Pearson correlation coefficients, we observed a notable correlation between four key metabolites (L-Isoleucine, L-Leucine, L-Valine, (R)−2,3-Dihydroxy-3-methylpentanoate) and three mobile Cmo mRNAs (*CmoCRLPK2*, CmoCh05G000400; *CmoEEIG1/EHBP1*, CmoCh06G005400; *CmoKARI1*, CmoCh19G010620) in cucumber leaves of the Csa/Cmo heterografts in response to chilling stress (Fig. 1e; Supplementary Data 7). Among them, *CmoKARI1* encodes an enzyme (ilvC, EC: 1.1.1.86) directly involved in the second step of parallel pathways leading to BCAA biosynthesis.

Our findings suggest that BCAA biosynthesis is likely a key metabolic pathway enriched with cold-induced directionally mobile mRNAs. Under normal conditions in Csa/Cmo heterografts, several cucumber mRNAs, including *CsaKARI, CsaIIL1/IPMI1/2*, *CsaAHAS1/CSR1*, *CsaDHAD*, *CsaIMS1* and *CsaTD1*, move from the Csa scion to the Cmo rootstock. Under cold conditions in Csa/Cmo heterografts, *CsaKARI, CsaIIL1/IPMI1/2*, *CsaAHAS1/CSR1*, *CsaDHAD*, *CsaIMD*, and *CsaTD1* move from the Csa scion to the Cmo rootstock (Fig. 1f; Supplementary Fig. 3a, b; Supplementary Data 8). To better understand the role of pumpkin as a rootstock in enhancing stress tolerance across diverse scion species, it is essential to focus on signals that originate directly from the pumpkin root. A criterion for such a signal is that it must be both transported to the scion and, ideally, responsive to environmental factors. Among the components of the BCAA pathway, CmoKARI1 is the only factor that meets these criteria. In contrast, although the other two genes also showed correlation, there are currently no reports suggesting a direct functional role (Supplementary Fig. 3b). Therefore, we prioritized the study of *CmoKARI1* in pumpkin-mediated chilling tolerance.

https://doi.org/10.1038/s41467-025-63228-1

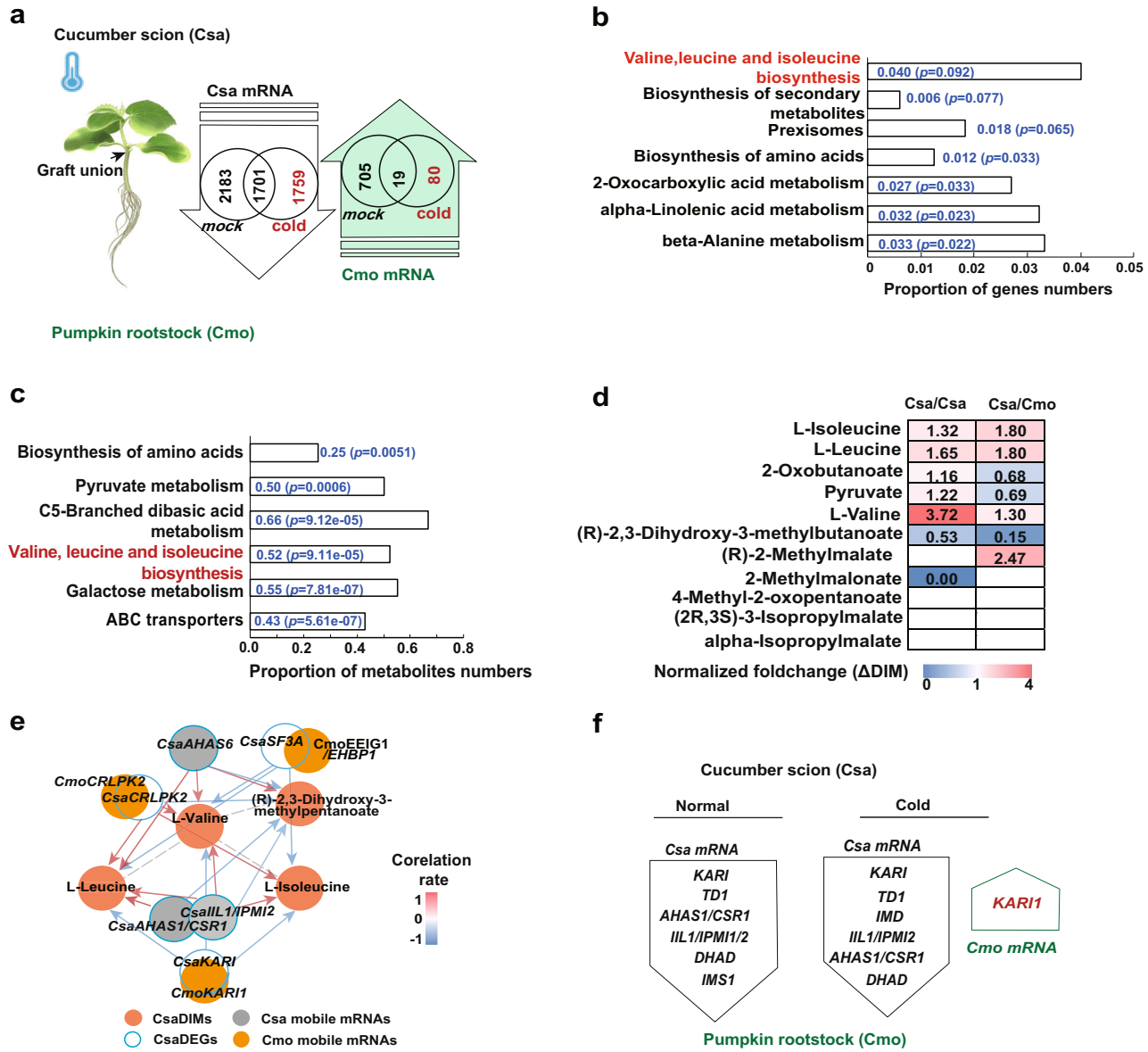

Fig. 1 | Analysis of mobile mRNAs between rootstock and scion under 6-hour chilling conditions. a Number and direction of mobile mRNAs exchanged between cucumber (Csa) scion and pumpkin (Cmo) rootstock under chilling stress. Move-down Csa mRNAs and move-up Cmo mRNAs are indicated by red letters. **b** KEGG enriched pathway analysis of 80 move-up Cmo mRNAs induced by cold stress. The red letters indicate the BCAA (Valine, leucine, and isoleucine) biosynthesis pathway, while the blue letters on the graphs represent the proportion of gene numbers and *p*-value. KEGG enrichment analyses were performed using Fisher's exact test ($p < 0.05$) and corrected for multiple comparisons by false discovery rate (FDR). **c** KEGG enriched pathway analysis of 174 CsaDIMs (differential intensity of metabolites) in the Csa scion of Csa/Cmo grafts under chilling stress compared to normal conditions. The red letters indicate the BCAA biosynthesis pathway, and the blue letters on the graphs represent the proportion of metabolite numbers and *P*-value. KEGG enrichment analyses were performed using Fisher's exact test ($p < 0.05$) and corrected for multiple comparisons by false discovery rate (FDR). **d** Normalized fold change of CsaDIMs in the Csa scion of Csa/Csa and Csa/Cmo under chilling stress compared to the same tissue under normal conditions. The square red-to-blue colored block indicates the normalized fold changes compared to Csa scion of Csa/Csa under normal conditions. **e** Networks of chilling-induced Cmo and Csa mobile mRNAs, Csa DEGs involved in the metabolites L-leucine, L-valine, and L-isoleucine biosynthesis. Red circles indicate the four metabolites, grey ones indicate Csa DEGs, blue circles indicate Csa mobile mRNAs, and orange ones indicate Csa DEG-coordinated homologous Cmo mobile mRNAs. Arrows (red for positive and blue for negative) indicate the correlation between metabolites and Csa DEGs. The correlation analysis was conducted using Pearson correlation coefficients ($|cor| \geq 0.95$, *P*-value < 0.05, two-sided). Source data are provided as a Source Data file. **f** Schematic showing mRNA mobility in the BCAA biosynthesis pathway in Csa/Cmo grafts.

CmoKARI1 mRNA, but not *CsaKARI1*, is transported from root to shoot upon chilling

The mobility of these identified mRNAs was validated using an established RT-PCR identification method for mRNA mobility in heterologous grafts[37] (Fig. 2a). To further validate the long-distance mobility of *CmoKARI1* in cucumbers, we cloned and constructed the full-length cDNA of *CmoKARI1* into an overexpression (OE) binary vector fused with GFP. These constructs were introduced into cucumber using the established hairy roots system[38]. RT-PCR analysis of the newly emerged leaves confirmed that *CmoKARI1* triggered the movement of *GFP* mRNA from transgenic roots to untransgenic new leaves under low temperature (Fig. 2b).

One critical question is whether, after the rootstock-to-scion transport of *CmoKARI1*, it can be translated in the destination tissues. Since the GUS protein exceeds the size of plasmadesmata and cannot be transported[38], we employed *CmoKARI1* fused with GUS reporter to

https://doi.org/10.1038/s41467-025-63228-1

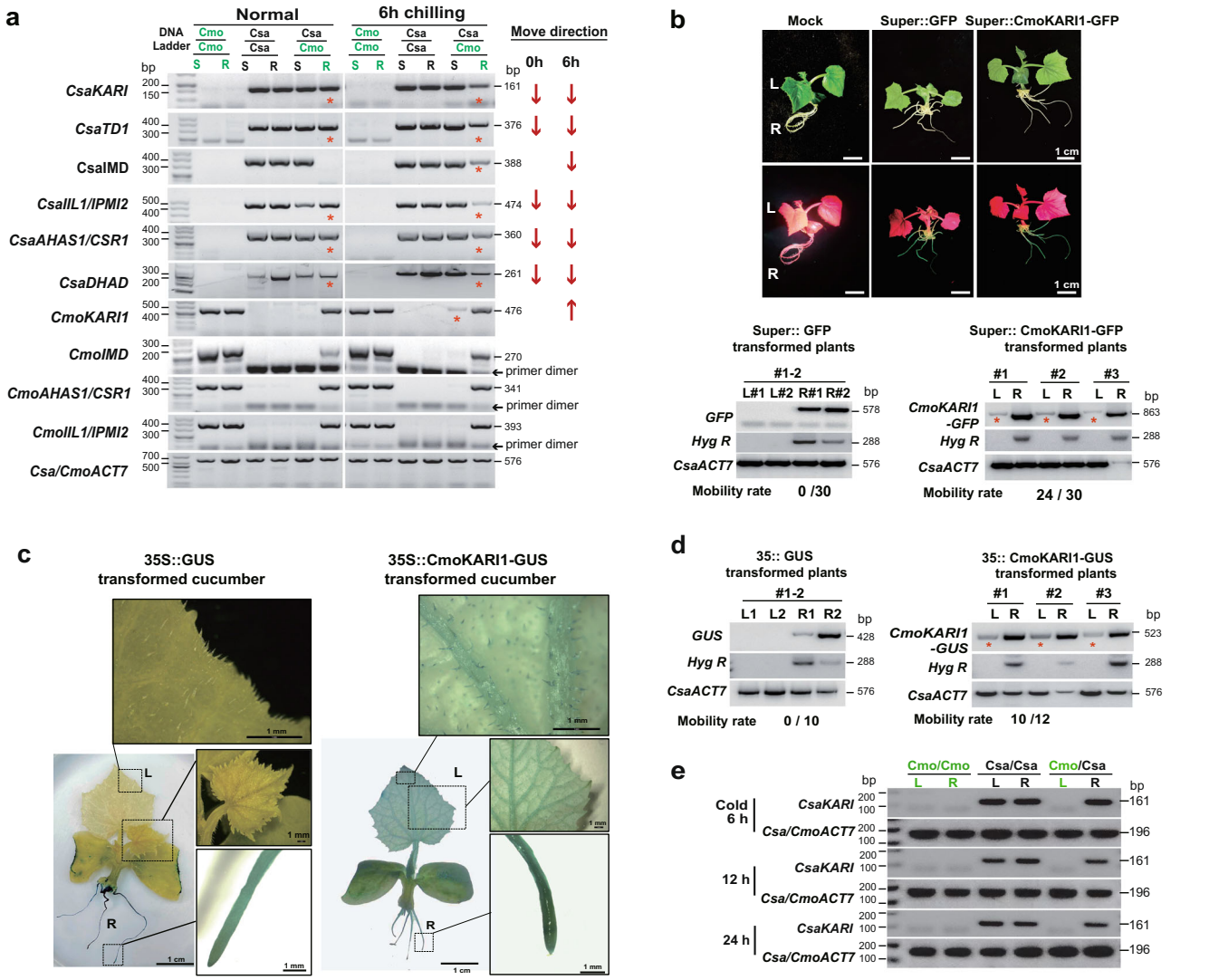

Fig. 2 | *CmoKARI1*, but not *CsaKARI*, exhibits upward movement and is translated by the cucumber scion in response to chilling stress. a RT-PCR identification of Csa and Cmo mRNA mobility under chilling conditions. Asterisks indicate mobile mRNAs identified in heterologous tissues. Arrows indicate movement direction. Cucumber or pumpkin *ACTIN7* was used as an internal reference for mRNA abundance. Lower bands that appeared were primer dimers serving as sample loading controls. See uncropped images in the source file. The samples derive from the same experiment, and the gels were processed in parallel. **b** Identification of *CmoKARI1* mobility from transformed cucumber hairy root to new leaves. The hairy root was transformed with cultures of *Agrobacterium rhizogenes* (Rhizobium rhizogenes) strain K599 harboring an empty vector (pCambia1300-Super::GFP) or pCambia1300-Super::CmoKARI1-GFP. K599 alone was transformed into a mock control. Fourteen days after transformation, RT-PCR with primers recognizing GFP was used to verify the mobility of *GFP* or *CmoKARI1-GFP*. #1, #2, and #3 represent independent transgenic seedlings as biological replicates. Mobility rate was analyzed by mobility seedlings/total independent hairy root transgenic seedlings. *CsaACTIN7* was used as an internal reference for mRNA abundance. *NPTII* was used to exclude the *Agrobacterium rhizogenes* contamination or mobility. GFP fluorescence was identified using the LUYOR-3415RG fluorescent protein lamp. The samples derive from the same experiment, and the gels were processed in parallel. **c** Mobile *CmoKARI1* from transformed cucumber hairy root was translated into new true leaves, shown by GUS staining. The hairy root was transformed with *Agrobacterium rhizogenes* (Rhizobium rhizogenes) strain K599 harboring an empty vector (pCambia1305-35S::GUS) or pCambia1305-35S::CmoKARI1-GUS. R: Agrobacterium-transformed cucumber hairy root, L: The emerged new leaves at 14 days after transformation. **d** RT-PCR with primers recognizing GUS was used to verify the mobility of *GUS* or *CmoKARI1-GUS*. #1, #2, and #3 represent independent transgenic seedlings as biological replicates. Mobility rate was analyzed by mobility seedlings/total independent hairy root transgenic seedlings. *CsaACTIN7* was used as an internal reference for mRNA abundance. The hygromycin resistance (Hyg R) gene was used to exclude *Agrobacterium rhizogenes* contamination or mobility. The samples derive from the same experiment, and the gels were processed in parallel. **e** RT-PCR identification of *CsaKARI* from cucumber rootstock to pumpkin scion at 6 h, 12 h, and 24 h under chilling conditions. R rootstock, L true leaves. The samples derive from the same experiment, and the gels were processed in parallel. Source data are provided as a Source Data file.

exclude the possibility of protein transport. Therefore, GUS staining can be used as an indication of local translation of imported mRNAs. By performing root transformation, we introduced *CmoKARI1* fused to a GUS reporter into cucumber roots. GUS staining indicated that the transported *CmoKARI1* mRNA could be translated into a functional protein in the scions upon chilling (Fig. 2c, d).

Interestingly, in the pumpkin scions grafted onto cucumber rootstocks, *CsaKARI* mRNA was unable to move to the scions upon chilling (Fig. 2e). We further characterized *KARI* genes in cucumber and pumpkin genomes. *CsaKARI* is a single-copy gene, and additional *CmoKARI2* (CmoCh11G019640) was identified (Supplementary Fig. 4a, b). They shared a high similarity of protein sequences, indicating their

https://doi.org/10.1038/s41467-025-63228-1

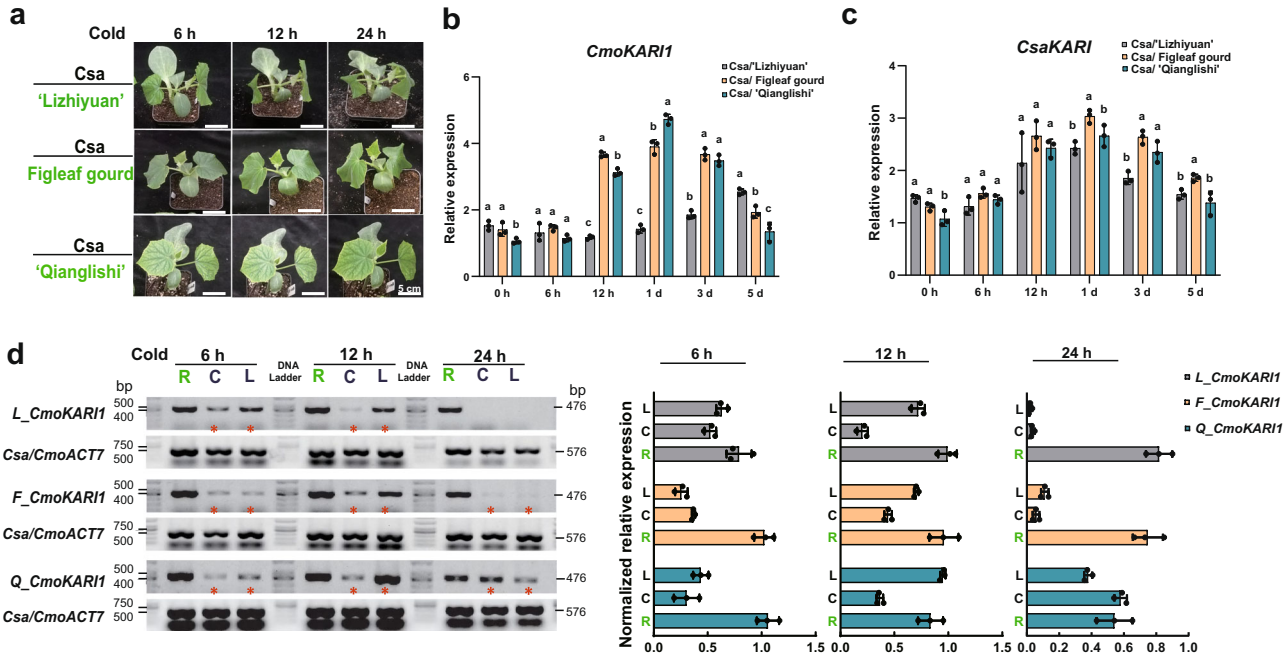

Fig. 3 | *CmoKARI1* moves from pumpkin root to cucumber shoot in response to chilling stress. a Phenotypic changes and **b, c** relative expression of *CmoKARI1* and *CsaKARI* in the leaf and root of grafted Csa/Cmo (Figleaf gourd, 'Qianglishi', and 'Lizhiyuan') under different time-course cold stress by qPCR. Each treatment includes $n = 3$ biological replicates, and each replicate includes 5 individual plants (mean ± s.d., one-way ANOVA followed by Duncan's test). Lowercase letters indicate significant differences ($p < 0.05$). Cucumber *ACTIN7* was used as an internal reference. **d** RT-PCR identification of *CmoKARI1* in grafted Csa/Cmo with pumpkin rootstock 'Lizhiyuan', Figleaf gourd and 'Qianglishi' at 6 h, 12 h, and 24 h under chilling conditions. R pumpkin rootstock, C cucumber cotyledons, L cucumber true leaves. The normalized relative expression of RT-PCR bands was analyzed by comparing with the corresponding *Csa/CmoACTIN7* using ImageJ software. Each treatment includes $n = 3$ biological replicates, and each replicate includes 5 individual plants (mean ± s.d.). Asterisks indicate mobile *CmoKARI1* in cucumber cotyledons and true leaves. The samples derive from the same experiment, and the gels were processed in parallel. Source data are provided as a Source Data file.

conserved catalytic activity. However, the transcript level of *CsaKARI* and *CmoKARI2* was not regulated by low temperature or heterografting (Supplementary Fig. 3b). In addition, *CmoKARI2* was not mobile in Csa/Cmo heterografts upon chilling (Supplementary Data 1). These findings suggest that the root-to-shoot mobility of *CmoKARI1* mRNA contributes specifically to the chilling tolerance of pumpkin as rootstocks, and excludes the potential role of *CsaKARI* and *CmoKARI2* in improving chilling tolerance of Csa/Cmo heterografts.

The root-to-shoot mobility of *CmoKARI1* is specifically associated with chilling-tolerant rootstocks derived from various pumpkin varieties

To investigate the impact of *CmoKARI1* long-distance movement on chilling responses and tolerance in grafted cucumbers, we used three different pumpkin varieties, including Figleaf gourd, 'Qianglishi,' and 'Lizhiyuan,' as rootstocks. All three pumpkin varieties as rootstocks significantly improved chilling tolerance in cucumber scions[5]. In our experimental system, we conducted a comprehensive analysis to assess the role of these three pumpkin rootstocks under chilling stress. Our findings categorized Figleaf gourd and 'Qianglishi' as chilling-tolerant rootstocks, while 'Lizhiyuan' exhibited lower chilling tolerance (Fig. 3a). Notably, the Csa/'Lizhiyuan' grafts displayed wilting and dehydration after 6 hours of chilling stress, whereas wilting was observed in Csa/'Qianglishi' and Csa/Figleaf gourd grafts after 3 days, respectively. Chilling Injury Index (CII), Relative Electrolyte Permeability (REP), and the expression of genes from the CBF-COR pathway confirmed comparable chilling tolerance in Csa/Figleaf gourd and Csa/'Qianglishi' grafts, with lower tolerance observed in Csa/'Lizhiyuan' grafts (Supplementary Fig. 5).

The expression analysis showed that the relative expression of *CmoKARI1* was induced in the chilling-tolerant pumpkin rootstocks, Figleaf gourd, and 'Qianglishi,' after 12 h and 1 day of chilling stress (one-way ANOVA followed by Duncan's test, $p < 0.05$). The mobility of *CmoKARI1* mRNA appears to be associated with the induced mRNA pool in the roots of chilling-tolerant pumpkin varieties. However, the relative expression of *CsaKARI* (CsGy7G004580) in cucumber scions was not influenced by different pumpkin rootstocks and only exhibited slight induction after 12 hours and 1 day of chilling stress (Fig. 3b, c). Since KARI controls BCAA biosynthesis, silencing the single-copy *CsaKARI* resulted in dwarf, chlorotic, and stunted cucumber seedlings, unsuitable for any further grafting or stress challenge (Supplementary Fig. 6a, d). Both REP and MDA levels indicated a markedly higher sensitivity to chilling stress in the *CsaKARI*-silenced line (Supplementary Fig. 6b, e). Due to the strong leaf chlorosis and waterlogging phenotype, the reference gene may no longer be reliable. This could explain the unexpected accumulation of *CsaCOR* and *CsaKARI* mRNAs following chilling stress in the silenced line (Supplementary Fig. 6c, f). These findings suggest that the non-cold-inducible *CsaKARI* likely provides a housekeeping function, while the chilling-inducible *CmoKARI1* from the rootstock appears to be required for improved chilling tolerance in the heterograft.

To confirm the movement of *CmoKARI1* mRNA to the cucumber scions, we conducted RT-PCR identification. We observed that *CmoKARI1* mRNA was transported from all rootstocks to the 1st–2nd true leaves and particularly the new leaves of cucumber scions after 6 h and 12 h of chilling stress. However, after 24 h of chilling stress, *CmoKARI1* mRNA was only detected in the scions of chilling-tolerant Figleaf gourd and 'Qianglishi' rootstocks. The chilling-sensitive 'Lizhiyuan' rootstock was no longer able to deliver *CmoKARI1* mRNA to the cucumber scions (Fig. 3d). Considering *CsaKARI* as a housekeeping system and *CmoKARI1* as the inducible one, an interesting question arises: what is the relative amount of *CmoKARI1* mRNA transported to the cucumber scion during chilling stress compared to *CsaKARI* mRNA transcribed in the scion? We re-analyzed the original RNA-seq data and found that

after 6 h of chilling stress, the amount of transported *CmoKARI1* mRNA reads in the scion was approximately 10% of the total *CsaKARI* transcripts (Supplementary Fig. 7; Supplementary Data 9). Importantly, transport of *CmoKARI1* mRNA increased and was even detectable after 36 h of chilling stress, the latest time point we could analyze before plant health declined (one-way ANOVA followed by Duncan's test, $p < 0.05$) (Supplementary Fig. 8). This suggests that *CmoKARI1* mRNA contributes significantly to the scion's BCAA pool alongside the scion's own *CsaKARI* expression.

The overexpression of *CmoKARI1* improves chilling tolerance of transgenic cucumber and *Arabidopsis thaliana*

CmoKARI1 knockout pumpkin rootstock would have allowed us to conclusively establish the essential role of mobile *CmoKARI1* in conferring cold tolerance to Csa/Cmo heterografts. However, pumpkin transformation is a technically demanding process with worldwide obstacles. Consequently, we employed root-transformation to introduce CmoKARI1-GFP/GUS into cucumber roots (Fig. 2), and evaluated its response to chilling stress. Notably, the overexpression of CmoKARI1–GFP/GUS in cucumber roots resulted in improved chilling tolerance after 12 h of chilling stress, as indicated by relative electrolyte permeability (REP) and malondialdehyde (MDA) content (Fig. 4a, b; Supplementary Fig. 9). Particularly, CmoKARI1–GUS protein is not capable of moving long-distance due to the size limitation of plasmodesmata[38]. These results further indicate that over-expressing *CmoKARI1* mRNA alone in the cucumber root is enough to confer chilling tolerance (Supplementary Fig. 9), excluding the possible involvement of protein transport.

KARI1 encodes an enzyme involved in the BCAA biosynthesis. To examine the significance of CmoKARI1-induced BCAA biosynthesis in the chilling tolerance of heterografts, we applied different concentrations of L-Leucine, L-Isoleucine, and L-Valine to the leaves of two-true-leaf-old cucumber seedlings (Supplementary Fig. 10). Following 12 h of cold treatment, it was observed that only 300 μM L-Isoleucine enhanced the cold tolerance of cucumber seedlings, as indicated by REP and MDA content (one-way ANOVA followed by Duncan's test, $p < 0.05$) (Fig. 4c, d). Interestingly, the application of L-Valine increased susceptibility to chilling, which aligned with the specific elevation of leucine and isoleucine levels, but not L-Valine, in the Csa/Cmo heterografts under chilling conditions (Supplementary Fig. 2c). These findings suggest the potential of L-Isoleucine application to modulate early chilling tolerance in cucumber, warranting further investigation.

To establish the relevance of *CmoKARI1* mobility and its impact on isoleucine biosynthesis in chilling tolerance, we introduced the constitutive expression of *CmoKARI1-GFP* into cucumber through stable transformation. Three independent lines with *CmoKARI1* transgenic lines (TG #1, #2 and #4) were selected based on genomic identification and transcription levels of *CmoKARI1* (Supplementary Fig. 11). After subjecting the cucumber plants to 12 h of 4 °C chilling stress, it was evident that overexpressed *CmoKARI1* significantly enhanced cucumber's chilling tolerance, and the exogenous application of L-isoleucine exhibited additive effects. The levels of MDA and REP in the *CmoKARI1* TG lines were lower than in the wild type, indicating improved chilling tolerance in both the *CmoKARI1* TG lines and through L-isoleucine application (one-way ANOVA followed by Duncan's test, $p < 0.05$) (Fig. 4e, f). Overexpression of *CmoKARI1* led to an increase in the endogenous isoleucine level, which correlated with the observed chilling tolerance phenotype (Fig. 4g, Supplementary Fig. 11a–i, Supplementary Fig. 12a–e). Additionally, the expression levels of *CsaCBF1* and *CsaCOR*, two key genes involved in cold response, were higher in the *CmoKARI1* TG lines compared to the wild type after 6 h of chilling stress (one-way ANOVA followed by Duncan's test, $p < 0.05$) (Supplementary Fig. 12f). Treatment with L-isoleucine further elevated the expression levels of *CsaCBF1* and *CsaCOR* in the *CmoKARI1* TG lines compared to the wild type and H_2O-treated TG seedlings (Fig. 4h). Furthermore, heterografs of WT and *CmoKARI1* TG cucumber lines exhibited stronger chilling tolerance compared to the self-rooted graft (Fig. 5a–c), with *CmoKARI1* moving from *CmoKARI1* TG rootstock into WT scion (Fig. 5d). These results collectively demonstrate that the overexpression of *CmoKARI1* in cucumber root and further its mobility to the shoot enhances cold tolerance in cucumber seedlings by promoting L-isoleucine biosynthesis.

To explore the broader effects of *CmoKARI1* and the potential application of L-isoleucine in improving cold tolerance in other plants, we also introduced *CmoKARI1* into *Arabidopsis* (Supplementary Fig. 13). Wild-type *Arabidopsis* Col-0 and two independent lines overexpressing *CmoKARI1* were treated with 50 μM and 100 μM L-isoleucine (Supplementary Fig. 13). Since Arabidopsis is far more cold-tolerant than cucumber, here we challenged Arabidopsis with freezing conditions. Although chilling and freezing stress are rather different, it is believed that all freezing-tolerant plants are also chilling-tolerant[39]. In the two independent transgenic *Arabidopsis* lines overexpressing *CmoKARI1* and supplied with L-isoleucine (Supplementary Fig. 13a–d), REP analysis revealed increased tolerance compared to the mock control (one-way ANOVA followed by Duncan's test, $p < 0.05$) (Supplementary Fig. 13e). Moreover, overexpression of *CmoKARI1* increased the content of L-isoleucine in transgenic Arabidopsis lines compared to the wild type after 4 days of recovery following freezing stress (Supplementary Fig. 13f). Additionally, elevated *JAZ1* expression indicated activation of the JA signaling pathway, consistent with the increased Ile levels (Supplementary Fig. 13f). Gene expression analysis in the Arabidopsis lines treated with 50 μM L-isoleucine showed similar results to cucumber seedlings, with higher expression levels of *AtCBF1* and *AtCOR15b* in the *CmoKARI1*ox lines compared to the wild type after chilling stress. Furthermore, when L-isoleucine was applied to the Arabidopsis lines, the expression levels of *AtCBF1* and *AtCOR15b* were even higher in the *CmoKARI1*ox lines compared to the wild type and H_2O-treated *CmoKARI1*ox seedlings (one-way ANOVA followed by Duncan's test, $p < 0.05$) (Supplementary Fig. 13g). These findings suggest that the function of overexpressed *CmoKARI1* in regulating isoleucine biosynthesis and influencing cold tolerance is conserved in both cucumber and *Arabidopsis*.

Root-to-shoot mobile *CmoKARI1* activates JA-Ile signaling

Different from valine and leucine, isoleucine plays a crucial role in synthesizing JA-Ile conjugates. It has been shown that Ile enhances abiotic stress resistance via the JA signaling pathway[40]. Therefore, we hypothesize that the delivery of *CmoKARI1* from the pumpkin rootstock to the cucumber scions during chilling stress enhances chilling tolerance by promoting the biosynthesis of isoleucine and JA-Ile, thereby activating JA-Ile signaling. After subjecting the plants to 12 h of chilling stress, the H_2O-treated *CmoKARI1* TG line exhibited greater cold tolerance than the wild type. Remarkably, the application of JA-Ile demonstrated an effect on chilling tolerance compared to JA or isoleucine treatment alone, as evidenced by both the phenotype and physiological parameters (one-way ANOVA followed by Duncan's test, $p < 0.05$) (Fig. 6a–c).

JA-Ile is synthesized by Jasmonoyl-L-amino acid synthetase 1 (JAR1)[41]. The JAR1 inhibitor Jarin-1 impaired chilling tolerance, particularly in the *CmoKARI1* TG lines (Fig. 6a–c). The expression level of *CsaCBF1* showed the highest induction upon JA-Ile treatment in the *CmoKARI1* TG lines, and this induction was abolished by Jarin-1 treatment (Fig. 6d). After 3-day chilling stress, JA-Ile application enhanced chilling tolerance in CmoKARI-GUS root transformed cucumber. In the presence of two JA-Ile biosynthetic substrates, JA and Ile, Jarin-1 impaired chilling tolerance and *CsaCBF1* expression (one-way ANOVA followed by Duncan's test, $p < 0.05$) (Supplementary Fig. 14). Further genetic evidence by silencing *JAR1* in the *CmoKARI1* TG lines under 3-day chilling conditions further supported the biosynthesis of JA-Ile determined the *CmoKARI1*-mediated chilling tolerance

https://doi.org/10.1038/s41467-025-63228-1

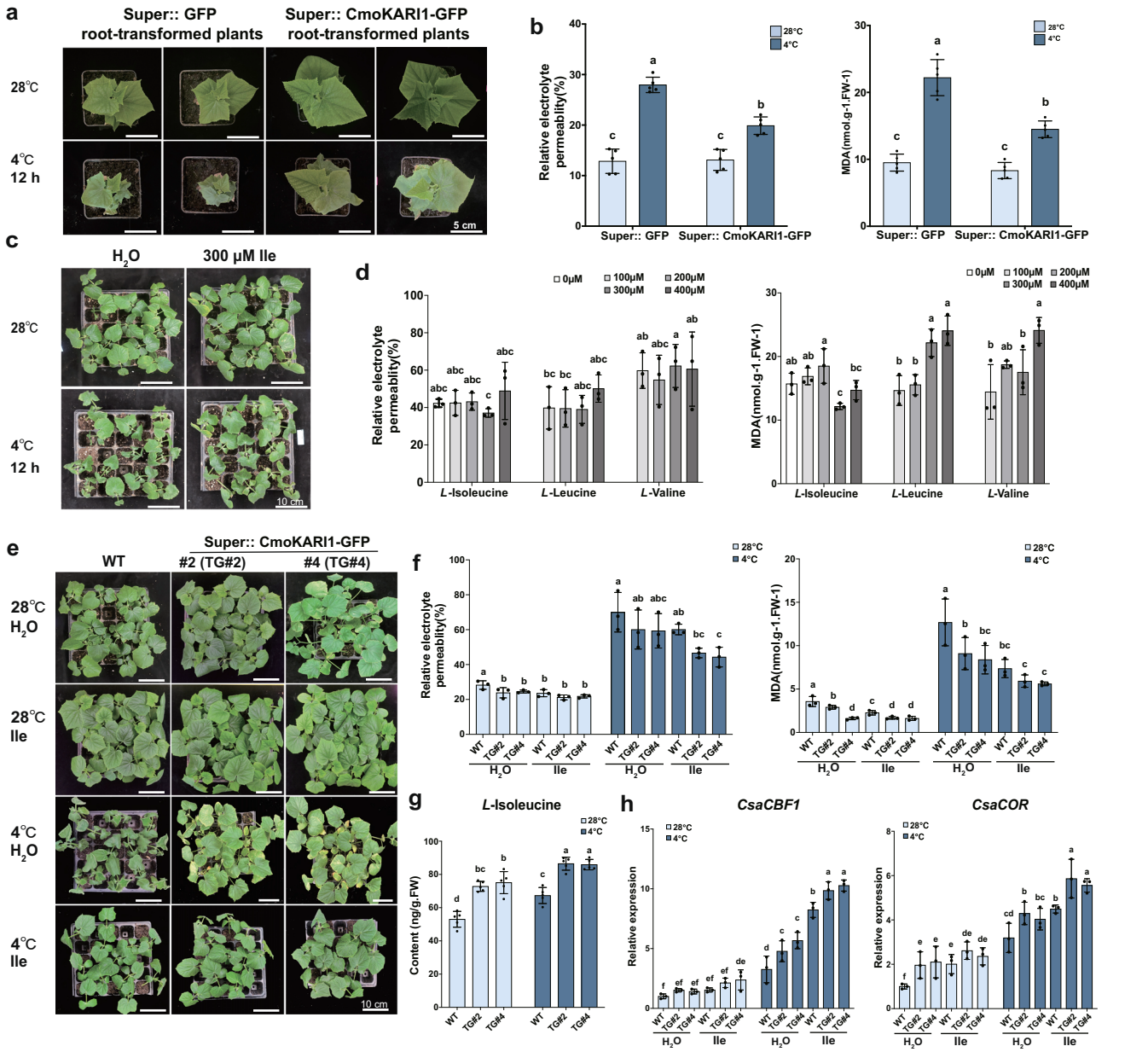

Fig. 4 | Move-up *CmoKARI1* improves cucumber chilling tolerance by inducing isoleucine biosynthesis. a Phenotypes, and **b** relative electrolyte permeability (REP) and MDA content of *CmoKARI1-GFP* root-transformed cucumbers after 12 h of 4 °C cold stress. **a**, **b** Each treatment includes 5 individual plants as $n = 5$ biological replicates (mean ± s.d., one-way ANOVA followed by Duncan's test). Lowercase letters indicate significant differences ($p < 0.05$). **c** Phenotypes, and **d** REP and MDA in two-leaf-old cucumber seedlings treated with 300 μM L-isoleucine before and after 12 hours of chilling conditions. The control group received H_2O. **c**, **d** At least $n = 3$ replicate pools were included, with each pool containing 12 plants, at both 0-h and 12-h chilling conditions (mean ± s.d., one-way ANOVA followed by Duncan's test). Lowercase letters on the graphs indicate significant differences ($p < 0.05$). **e** Phenotypes, **f** REP and MDA content, **g** isoleucine content, and **h** Relative expression of *CsaCBF1* and *CsaCOR* in two-leaf-old Super::CmoKARI1-GFP transgenic (TG) lines (TG#2 and TG#4) and wild-type cucumber seedlings before and after 12 h of chilling conditions. Cucumber *ACTIN7* was used as an internal reference. The control group received H_2O. Each treatment includes $n = 3$ (**f**, **h**), $n = 5$ (**g**) biological replicates, and each replicate includes 12 individual plants (mean ± s.d.), for each condition (one-way ANOVA followed by Duncan's test for the 28 °C and 4 °C groups). Source data are provided as a Source Data file.

(Supplementary Fig. 15). Notably, isoleucine treatment increased the expression of *CsaJAR1*, suggesting an enhanced JA-Ile synthesis in response to the availability of biosynthetic precursors (Fig. 6d).

While JA can be used to synthesize either JA-Ile or MeJA, our findings indicate that MeJA's effect on chilling tolerance is much less significant compared to JA-Ile (Fig. 6e). Intriguingly, the *CmoKARI1* TG line treated with MeJA exhibited increased sensitivity compared to the MeJA-treated wild type or H_2O-treated *CmoKARI1* TG cucumber lines (Fig. 6a). This result highlights the specific role of JA-Ile, rather than other forms of JAs, in cucumber's chilling tolerance. Consistently, MeJA levels decreased in the wild type upon cold treatment, while JA-Ile levels, especially in the *CmoKARI1* TG line, increased (Fig. 6e). We further confirmed elevated levels of both Ile and JA-Ile in Csa/Cmo heterografts compared to control self-rooted grafts (Supplementary Fig. 16a), and in *CmoKARI1* TG cucumber compared with WT (Supplementary Fig. 12c, d). Additionally, both heterografts and *CmoKARI1* TG lines exhibited increased transcript levels of the JA-signaling genes *JAZs*, *MYC2*[42], and *CBF1*[14] (Supplementary Fig. 12e, f).

In conclusion, our findings suggest that *CmoKARI1* mRNA is specifically delivered from pumpkin rootstocks to cucumber scions in

https://doi.org/10.1038/s41467-025-63228-1

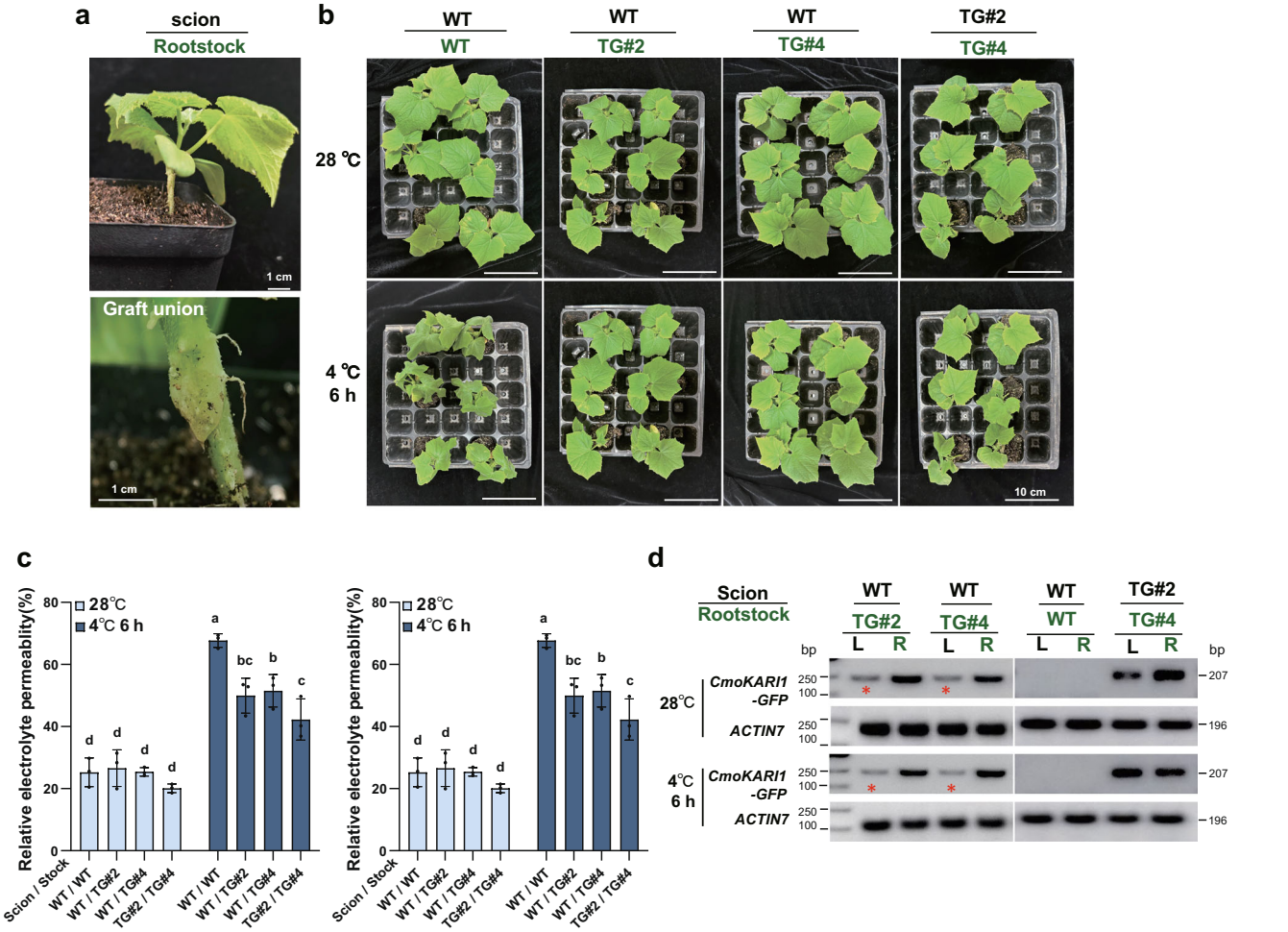

Fig. 5 | The rootstock-to-scion mobility of *CmoKARI1* mRNA confers cucumber chilling tolerance. a The two-leaf-old wild-type cucumber seedlings grafted onto Super::CmoKARI1-GFP transgenic (TG) lines (TG#2 and #4) and wild-type cucumber seedlings transgenic lines. The lower panel image showed the graft union. Each graft combination includes $n = 9$ individual grafted plants. **b** Phenotypes of the two-leaf-old wild-type cucumber seedlings grafted onto Super::CmoKARI1-GFP transgenic lines (TG) (TG #2 and #4) and wild-type cucumber rootstocks before and after 6 h of chilling conditions. **c** Relative electrolyte permeability (REP) and MDA content of wild-type grafted onto TG #2/#4 and wild-type cucumber rootstocks at 6 h of chilling conditions. Each treatment includes three biological replicates, with 3–4 individual plants per replicate (mean ± s.d., one-way ANOVA followed by Duncan's test, $p < 0.05$). Significance analysis of REP and MDA content was performed in separate groups at 28 °C and 4 °C. **d** RT-PCR identification of *CmoKARI1-GFP* in grafted WT/WT, WT/TG#2 and WT/TG#4 before and 6 h chilling conditions. R Rootstock, L Cucumber wild-type scion, Asterisks indicate movement fusion mRNA of *CmoKARI1-GFP*. $n = 3$ replicates were included, with each containing nine individual plants. Cucumber *ACTIN7* was used as an internal reference. The samples derive from the same experiment, and the gels were processed in parallel. Source data are provided as a Source Data file.

response to low temperatures. Once translated, CmoKARI1 participates in isoleucine biosynthesis, which further promotes the biosynthesis of JA-Ile and activates JA-Ile signaling to cope with chilling stress (Fig. 6f).

Although mobile *CmoKARI1* significantly enhances chilling tolerance in heterografts, it is essential to distinguish the effects of CmoKARI1-mediated local Ile biosynthesis from potential Ile transport from pumpkin root to cucumber scions. To address this, we treated Csa/Cmo heterografts with FITC-labeled Ile and measured the relative signal intensities. Pumpkin root showed a greater uptake and transport capacity of Ile and Leu compared to cucumber root; however, the rate of Ile and Leu transport decreased to almost the background level under chilling stress (Fig. 7a–c). These findings suggest that the increased Ile levels observed in *CmoKARI1* TG lines and Csa/Cmo heterografts likely result from CmoKARI1-mediated local Ile biosynthesis.

Discussion

Pumpkin is extensively used as a rootstock for grafting cucurbit crops, with the aim of enhancing yield and stress tolerance in the scions. Pumpkin rootstocks induce various phenotypic and physiological changes in the scions, including the regulation of nutrient homeostasis, alteration of endogenous hormones, and maintenance of photosynthesis and antioxidant capacity[3,6]. However, there is a lack of comprehensive research on the mobile root-borne signals, and the underlying mechanism remains largely unknown. In this study, we made an important discovery by identifying a specific mRNA molecule, *CmoKARI1*, which is transported exclusively from the pumpkin rootstock to the cucumber scion under chilling stress conditions (Figs. 1 and 2). Particularly, when cucumber was used as a rootstock, the corresponding mRNA molecule in cucumber (*CsaKARI*) did not exhibit upward movement (Fig. 2e). These findings establish a significant mechanistic connection between pumpkin rootstock and the stress tolerance of grafted cucurbit crops.

The transportation of mobile RNAs is primarily known to occur from shoot to root through the phloem, alongside the movement of photosynthates[34,35]. However, this mechanism alone does not fully explain the role of pumpkin as a rootstock. In this study, we made an intriguing discovery of *CmoKARI1* being transported from the pumpkin

https://doi.org/10.1038/s41467-025-63228-1

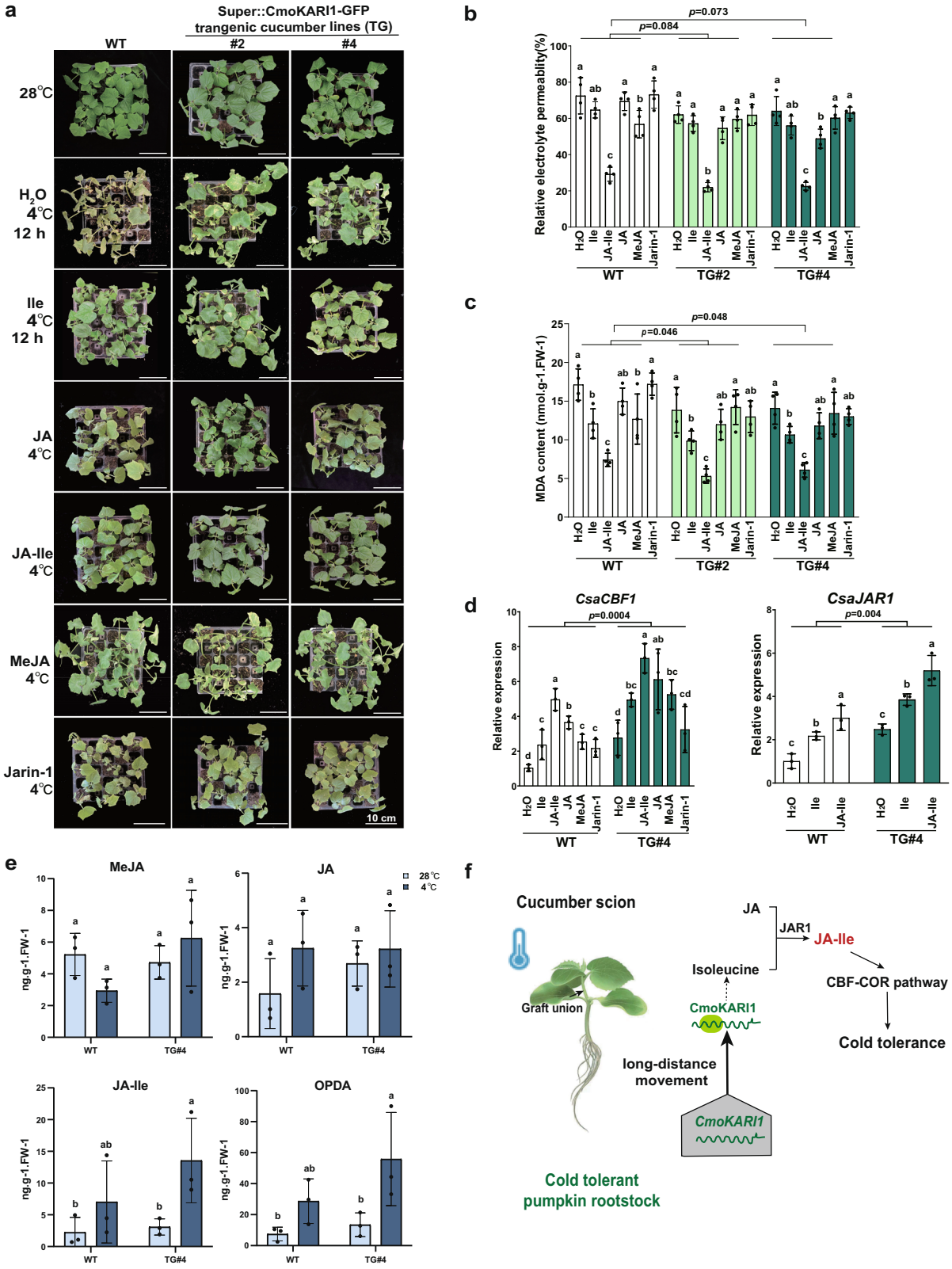

root to the scion, specifically under chilling stress conditions. This finding suggests that the xylem, which is responsible for water and nutrient transport, may play a crucial role in mRNA transport. While Buhtz et al. previously reported the absence of RNAs in the xylem of Brassica plants[42], subsequent studies have identified various mRNAs and non-coding RNAs in micro-dissected xylem samples[43]. Additionally, RNA m^5C modification has been extensively studied and found to regulate RNA mobility[28]. Interestingly, in our investigation using the Cucume database of RNA mobility and methylation, we observed that mobile *CmoKARI1* exhibited m5C modification only in the vascular samples, but not in the samples from the whole plants[44]. The precise mechanism by which the chilling signal triggers the specific loading of *CmoKARI1* into the xylem for its long-distance transport remains unclear. However, the mobility of *CmoKARI1* demonstrated a positive

Fig. 6 | Move-up *CmoKARI1* improves cucumber chilling tolerance by specifically inducing the JA-Ile signaling pathway. a Phenotypes, **b** Relative electrolyte permeability (REP), and **c** MDA content in two-leaf-old Super::CmoKARI1-GFP transgenic (TG) and wild-type cucumber seedlings treated with H_2O control, 300 μM Ile, 100 μM JA, 200 μM MeJA, 100 μM JA-Ile, and 200 μM Jarin-1 before and after 12 h of chilling conditions. H_2O was used as the control. $n = 4$ replicate pools were included, with each pool containing 12 plants, for each treatment (mean ± s.d., one-way ANOVA followed by Duncan's multiple comparisons test within each genotype, $p < 0.05$; *p*-values at the top indicating the statistical difference between genotypes within each treatment group determined by one-way ANOVA). **d** Relative gene expression levels of *CsaCBF1* and *CsaJAR1* in the first true leaf under different growth conditions. Each treatment includes $n = 3$ biological replicates, with 12 individual plants per replicate (mean ± s.d., one-way ANOVA followed by Duncan's multiple comparisons test within each genotype, $p < 0.05$; *p*-values at the top indicating the statistical difference between WT and TG within each treatment group determined by Student *t*-test). Cucumber *ACTIN7* was used as an internal reference. **e** Content of JA, MeJA, JA-Ile, and OPDA was determined in wild-type (WT) and Super::CmoKARI1-GFP transgenic (TG#4) under 28 °C and 4 °C conditions. Each treatment includes $n = 3$ biological replicates, with 4 individual plants per replicate (mean ± s.d., one-way ANOVA followed by Duncan's test, $p < 0.05$). **f** Schematic model depicting the improvement of cold tolerance in cucumber scion under cold stress through the pumpkin rootstock-derived mobile *CmoKARI1*. The long-distance movement of *CmoKARI1* accelerates isoleucine biosynthesis, providing substrates for JA-Ile biosynthesis controlled by *CsaJAR1*. The accumulation of JA-Ile activates the CBF-COR pathway, thereby enhancing chilling tolerance in cucumber. Source data are provided as a Source Data file.

correlation with the chilling tolerance of different pumpkin breeding varieties (Fig. 3a–d). This correlation suggests that different pumpkin breeding varieties could serve as a valuable genetic tool for further exploration and identification of communication factors involved in transmitting root-to-shoot signals in response to environmental cues.

KARI1 encodes a critical enzyme involved in the synthesis of branched-chain amino acids (BCAAs). Studies have shown that mutating other genes involved in BCAA biosynthesis, such as *IIL1*/*IPMI1*, results in growth defects and increased sensitivity to cold temperatures[44,45]. This suggests that BCAAs play an important role in plant cold tolerance. During low temperatures, energy production in plants is often limited. BCAAs are physically connected to the mitochondrial respiratory chain, which regulates energy metabolism[46]. In eukaryotes, BCAAs are known to activate the target of rapamycin (TOR) kinase, a master energy sensor[47,48]. TOR integrates various environmental signals and coordinates transcription and translation[49,50]. Under cold stress, TOR activity is rapidly diminished after 2 h but recovers after 24 h[51]. In fact, silencing of TOR has been shown to lead to heightened sensitivity to cold conditions[52]. The increased isoleucine levels, possibly resulting from Csa/Cmo heterografts, could potentially activate TOR kinase and benefit plants under chilling conditions. Recent research has also highlighted the importance of TOR in shoot-root communication during abiotic stress[53]. A future challenge will be to investigate whether the mobile *CmoKARI1*-mediated isoleucine biosynthesis is required for TOR activation and how TOR enhances chilling tolerance in grafted crops. Understanding these mechanisms will contribute to a more comprehensive understanding of the role of BCAAs, TOR kinase, and root-to-shoot signaling in improving the cold tolerance of grafted crops.

Intriguingly, when only isoleucine was sprayed, and not other BCAAs, the chilling tolerance of cucumber was enhanced (one-way ANOVA followed by Duncan's test, $p < 0.05$) (Fig. 4). This finding suggests that isoleucine, among the BCAAs, plays a crucial role in promoting chilling tolerance. One notable distinction between BCAAs is that isoleucine is involved in the synthesis of JA-Ile conjugates. JA signaling is known to be relevant for plants in coping with low temperatures[11]. A previous study showed that applying Ile enhances JA-Ile-dependent Botrytis resistance[40]. JA signaling is known to be relevant for plants in coping with low temperatures[11]. JA-Ile, JA, and the precursor OPDA have been shown to be mobile, facilitating shoot-to-root coordination in response to wounding. Importantly, it is worth noting that JA-Ile and its biosynthetic precursors are capable of moving downward, likely following the phloem stream along with photosynthates. However, they are unable to move upward in *Arabidopsis*[19]. This excludes the possibility of pumpkin rootstocks delivering JA-related metabolites to the scion. Recently, we identified that *CmoCK1* mRNA is specifically transported from pumpkin rootstock to cucumber scion in response to chilling stress. CK1 plays a role in JA biosynthesis, which further supports the concept of local JA biosynthesis within the scion, rather than long-distance transport from the rootstock[51]. Consequently, our conclusion is further reinforced that *CmoKARI1* is the key communication molecule responsible for inducing local biosynthesis of JA-Ile in the grafted scion.

A significant limitation of this study is the inability to definitively establish a causal relationship between *CmoKARI1* mRNA transport and chilling tolerance in the scion. The lack of loss-of-function mutants in pumpkin, due to technical constraints, prevents a more conclusive assessment. This limitation leaves open the possibility that other systemic signals, such as metabolites, proteins, or small RNAs, may also contribute to chilling tolerance in the scion. For instance, gamma-aminobutyric acid (GABA) has been implicated in heterograft chilling tolerance, as FITC-labeled GABA exhibited a higher transport rate from pumpkin rootstock to cucumber scion under chilling stress[54]. In contrast, the transport of Ile and Leu was less pronounced under chilling conditions (Fig. 7a–c), supporting the notion that increased Ile and Leu levels in the heterograft during chilling are primarily due to local synthesis. Notably, Ile, but not Leu, specifically enhances chilling tolerance via the JA-Ile pathway. Further research is needed to elucidate how GABA and JA-Ile coordinate responses to chilling stress. It is important to acknowledge that FITC labeling is not an entirely accurate quantitative method. The use of high concentrations of labeled metabolites may result in non-physiological transport behavior[54]. Thus, determining the mobility of metabolites under physiological conditions remains a technical challenge that requires further methodological advancements.

Overall, our results unveil a notable case where *CmoKARI1* mRNA is transported from the pumpkin rootstock to the grafted scion, specifically under chilling stress conditions. While researchers generally believed that the enhanced stress tolerance conferred by pumpkin rootstock was primarily attributed to its robust root system, our findings suggest that pumpkin rootstock is capable of delivering specific mobile molecules in response to distinct environmental cues. This discovery not only identifies an important mobile mRNA target for future crop breeding but also provides unprecedented insights into grafting biology.

Methods

Plant materials, growth conditions, grafting and chilling treatment

Cucumber (*Cucumis sativus* L. 'Xintai Mici') (Csa) was used as the scion, while pumpkin (*Cucurbita moschata* 'Qianglishi', 'Lizhiyuan', Shouguang Hongliang Seed Co.) and pumpkin (*Cucurbita ficifolia* Bouché.) (Cmo) were used as rootstocks. The grafting combinations included Csa/Cmo, Cmo/Csa, Csa/Csa, and Cmo/Cmo. Grafted plants were initially kept in complete darkness for 3 days in a growth chamber maintained at 28 °C and 100% relative humidity. This was followed by another 4-day period under low light conditions (16 h light/8 h dark; light intensity: 60–100 μmol m^{-2} s^{-1}) in a growth chamber with a 28 °C/18 °C day/night temperature regime and 90% relative humidity. Seven days post-grafting, the formation of the graft union was evaluated after removing the grafting clip.

https://doi.org/10.1038/s41467-025-63228-1

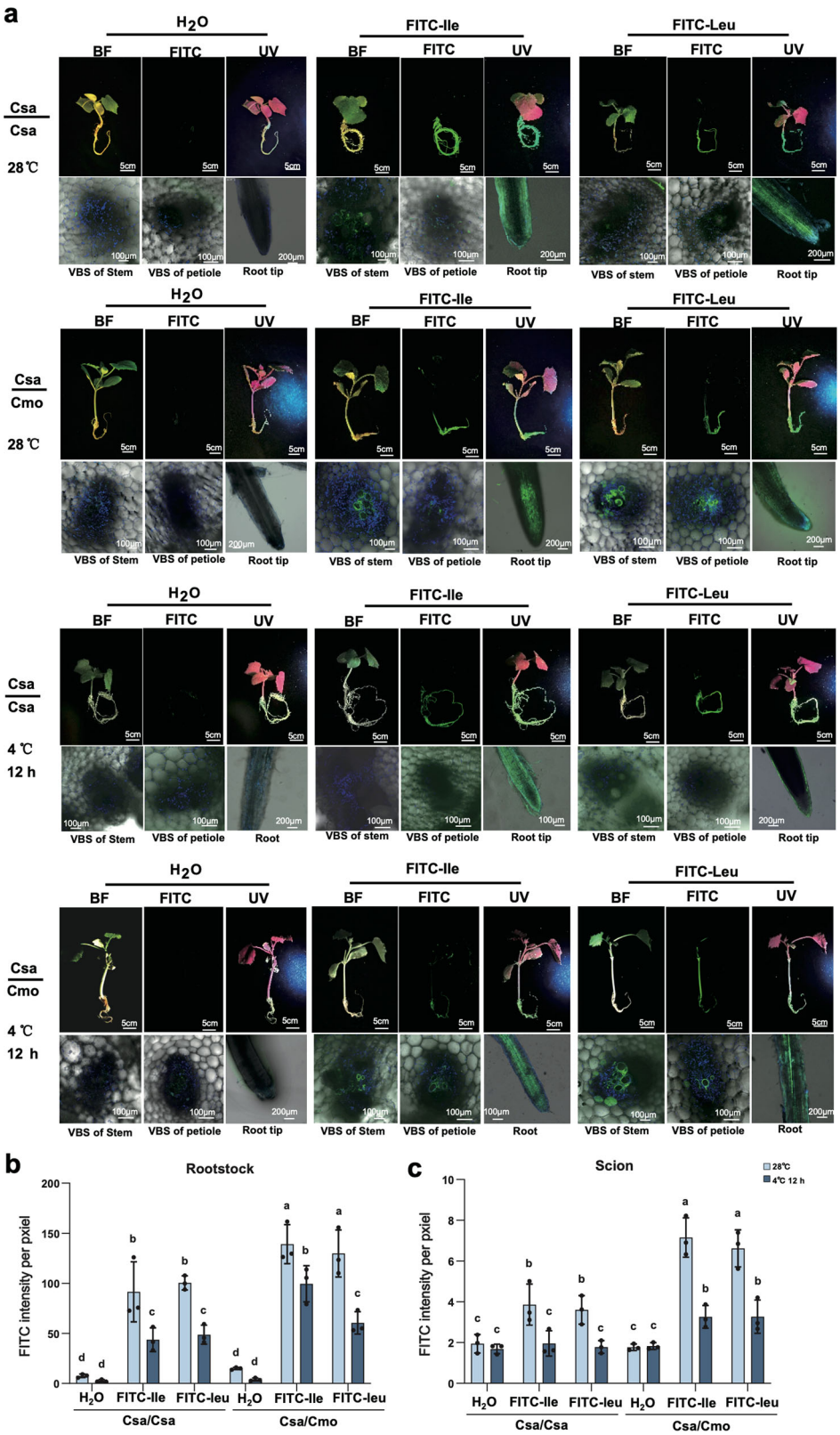

For chillin treatment, either cucumber plants or 7-day post-grafted cucumbers were transferred to a growth chamber under chilling stress conditions (4 °C; 16 h light/8 h dark; light intensity: 60–100 μmol m^{-2} s^{-1}; relative humidity: 70%). For metabolites application treatment, cucumber seedlings were cultured in a growth chamber (28 °C/18 °C 16 h/8 h day/night; light intensity: 200 μmol m^{-2} s^{-1}; relative humidity: 60%) in a mixed matrix (peat:vermiculite:perlite = 2:1:1, by vol.) until they were two-leaf old. Approximately 100–200 seedlings were subjected to treatment by spraying them twice per day with 25 ml of a water solution containing either 0, 100, 200, 300, or 400 μM L-leucine, L-isoleucine, and L-valine (Sigma-Aldrich, Shanghai, China). Alternatively, seedlings were sprayed twice per day with a water solution containing 100 μM JA (TCI, Shanghai, China), 100 μM MeJA (Sigma-Aldrich, Shanghai, China),

Fig. 7 | Uptake and transport of FITC-Isoleucine (Ile) and FITC-Leucine (Leu) from pumpkin (Cmo) rootstock to cucumber (Csa) scion under chilling stress. **a** Bright-field and fluorescence images of grafted plants, roots, stems, and petioles of Csa/Csa and Csa/Cmo plants after root irrigation with 50 μM FITC-Ile and FITC-Leu under normal (28 °C) and cold stress (4 °C for 12 h) conditions. H_2O was used as the control. BF bright-field images, FITC fluorescence images of FITC-Ile and FITC-Leu (channel RGB = 0:18:0) manually extracted using ImageJ, UV fluorescence detected using a LUYOR-3415RG fluorescent protein lamp. Fluorescence images of roots and vascular bundle sheath (VBS) cells in stem cross-sections and petioles were captured using a confocal laser scanning microscope (TCSSP8, Leica) with an excitation wavelength of 488 nm. Three individual plants were analyzed per treatment. **b**, **c** Statistical analysis of FITC fluorescence intensity per pixel, quantified using ImageJ software. Each treatment includes $n = 3$ biological replicates, with 5 individual plants per replicate (mean ± s.d.). Statistical significance was determined by one-way ANOVA followed by Duncan's multiple comparisons test with the wild type as the control ($p < 0.05$). Source data are provided as a Source Data file.

100 μM JA-Ile (Macklin, Shanghai, China), or 100 μM Jarin-1 (Macklin, Shanghai, China). After three days, all seedlings were transferred to 4 °C with normal light and humidity. Physiological traits of the seedlings were assessed at two time points: 0 h (non-chilled control) and after 12 h of chilling treatment. For each condition, the leaves of 5–6 randomly selected individual plants were harvested and combined into one replicate pool. At least three replicate pools were collected for each condition to perform further analysis of physiological traits and quantitative RT-PCR (RT-qPCR) assays.

Chilling treatment of *Arabidopsis thaliana* (Col-0) was performed, with modification. Surface sterilization of wild type (Col-0) and overexpressed (TG) seeds was performed using 70% ethanol solution and 5% NaClO solution, and grown on 1/2 MS medium. The seeds were then placed in a growth chamber at 22 °C for 8–10 days till seedling growth. Chilling treatment was performed at −10 °C freezing room for 1 h, then cultured under 22 °C growth chamber (12 h/12 h day/night; light intensity: 200 μmol m^{-2} s^{-1}; relative humidity: 60%) for 2 days and 4 days, and then the phenotypes, survival rate and cold tolerance were determined.

Cucumber and *Arabidopsis* transformation

A 1773-bp PCR fragment containing the complete coding sequence of *CmoKARI1* was obtained from the Cucurbit Genomics Database (*Cucurbita moschata* (Rifu) Genome). The fragment was amplified from pumpkin 'Qianglishi' cDNA using specific primers (Supplementary Table 1) and subsequently cloned into the pGEM-T Easy (TaKaRa, Beijing, China) vector. The open reading frame of *CmoKARI1* was inserted into the Super promoter-derived GFP-fused binary vector *pCambia1300* using XbaI/SalI restriction digestion sites. It was also inserted into the 35S promoter-derived GUS-fused binary vector, a modified version of *pCambia1305.1*, using XbaI/BamHI restriction digestion sites. Either the recombined vector *pCambia1305*-p35S::CmoKARI1-GUS or *pCambia1300*-pSuper::CmoKARI1-GFP was transformed into cucumber hairy roots of the cultivar 'Xintaimici' through *Agrobacterium tumefaciens* (K599)-mediated cucumber hairy root transformation with modification[53]. The seeds were immersed in 55 °C water for 30 min, and the seed coats were removed. After surface-sterilization with 70% ethanol for 30 s and 3% sodium hypochlorite for 8 min, they were sown onto MS medium and incubated at 28 °C in the dark for 4 d. A. rhizogenes strain K599 grown to an OD600 of 0.8–1.0 is pelleted by centrifugation and re-suspended in MS liquid medium supplemented with 200 μM Acetosyringone (CA1061, Beijing Coollab Technology Co., Ltd.) for infection. After inoculation, explants are co-cultivated in the dark at 25 °C for 3 d. Following co-cultivation, the hypocotyl of each explant is inserted into rooting medium and cultured under a 16 h light/8 h dark photoperiod to induce hairy-root formation. Transgenic roots are identified by GFP epifluorescence under Fluorescent Protein Lamp (LUYOR-3415RG, Shanghai Luyor Instrument Co., Ltd.). The *Agrobacterium tumefaciens* (GV3101) containing the recombined vector *pCambia1300*-pSuper::CmoKARI1-GFP fused binary vector was used to transfect *Arabidopsis thaliana* (Col-0) and cucumber cotyledon. Transgenic lines were screened in a selection medium and verified at the DNA and RNA levels through PCR and RT-qPCR. T2 transgenic lines were used for further study. The primers used for cloning, construction, and PCR are listed in Supplementary Table 1.

REP and MDA measurement

Relative electrolyte permeability (REP) and malondialdehyde (MDA) content were assessed following the method with some modifications[7]. To measure REP, leaf discs were immersed in distilled water at room temperature. The initial electrical conductivity of the distilled water was measured and recorded as EC_0. After shaking for 2.5 h, the electrical conductivity of the solution was measured again and designated as EC_1. The samples were then incubated in a 95 °C water bath for 30 min, cooled to room temperature, and the final electrical conductivity was recorded as EC_2. The relative electrolyte leakage was calculated using the formula: $(EC_1 - EC_0)/(EC_2 - EC_0) \times 100\%$. Malondialdehyde (MDA) content thiobarbituric acid (TBA) method. Fresh leaf tissue was homogenized in trichloroacetic acid (TCA) using a pre-chilled mortar and pestle. The absorbance of the supernatant was measured at 532 nm and corrected for nonspecific turbidity by subtracting the absorbance at 600 nm. The MDA concentration was calculated using an extinction coefficient of 155 mM^{-1} cm^{-1} and expressed as nmol MDA per gram of fresh weight (nmol g^{-1} FW).

For each graft combination, three to five individual cucumber seedlings and 7–10 leaf disks per leaf were harvested and pooled into three replicates at each chilling treatment time point for subsequent analysis. Similarly, for each transgenic *A. thaliana* line, three pools, each consisting of 10 individual seedlings with similar growth status, were harvested at each chilling treatment time point.

RT-PCR and RT-quantitative PCR

Total RNA was extracted from the entire first leaf and root using a FreeZol Reagent kit (R711-01, Vazyme Biotech Co., Ltd., Nanjing, China). Reverse transcription reactions were performed using a HiScript IV All-in-One Ultra RT SuperMix kit (Vazyme Biotech Co., Ltd., Nanjing, China, Cat#R433-01) following the manufacturer's instructions with the following steps: total RNA (~1 μg) treated with 5 μL 4× All-in-One Ultra qRT SuperMix. The reaction program was as follows: 50 °C for 5 min, followed by 85 °C for 5 s.

Quantitative RT-PCR was performed according to the SYBR method in a 10-μL volume using 20 ng total RNA, 5 μL Taq Pro Universal SYBR qPCR Master Mix (Vazyme Biotech Co., Ltd., Nanjing, China, Cat#Q712-02) and 0.2 μl forward and reverse primers. Each sample comprised RNA isolated from 3 to 5 individual plants. At least three technical replicates were performed. An ABI System Sequence Detector (QuantStudio™ 6 Flex real-time PCR system, CA, United States) was used with the following thermal cycling conditions. Stage 1: 1 cycle at 95 °C for 30 s; Stage 2: 40 cycles at 95 °C for 10 s, 60 °C for 30 s; Dissociation stage: 15 s at 95 °C, 1 min at 60 °C, 15 s at 95 °C. After amplification, melting curve analysis was performed to verify the product. Measured Ct values were converted to relative copy numbers using the ΔΔCt method. Each sample comprised RNA isolated from 3 to 5 individual plants. At least three technical replicates were performed. Values were normalized by using *CmoActin* or *CsaActin*. Primers are listed in Supplementary Table 1.

Identification of mobile mRNAs by RNA-seq and RT- PCR

Based on the nonsense consensus genomes of Csa (*'Xintaimici'*) and Cmo (*'Qianglishi'*), the detailed strategy of mobile mRNA calling was performed based on Single Nucleotide Polymorphism (SNP) comparison with consensus Cmo-modified and a Csa-modified genome using bcftools 1.8-1 software[36,37]. Lists of mobile mRNA datasets were generated for both no chilling and 6 h chilling conditions using the Tophat v2.2 and BLASTn programs. The verification of mRNA mobility by RT-PCR was performed using established technology[36,37]. RT-PCR assays on RNA samples of all homo- and heterograft combinations using primers designed to recognize specific sequences of Csa/Cmo transcripts with 2xRapid Taq Master Mix (Vazyme Biotech Co., Ltd., Nanjing, China, Cat#P222-03). Stage 1:1 cycle at 95 °C for 3 min; Stage 2: 40 cycles at 95 °C for 15 s, 60 °C for 15 s, 72 °C for 15 s/kb; Stage 3: 5 min at 72 °C. The primer used in this study was listed in Supplementary Table 1.

Integrative analysis of metabolites and transcripts

KEGG pathway and Venn analyses of DIMs or DEGs were both performed with the OmicShare tools (http://www.omicshare.com/tools). The corresponding numbers of DEGs from the FPKM values were performed as follows: (i) The difference in transcript abundance in the same tissue between heterologous and homologous grafts without chilling, i.e., fold difference of FPKM value (control Csa/Cmo leaf − control Csa/Csa leaf), was recorded as Δ1. (ii) The difference in transcript abundance in the same tissue between heterologous and homologous grafts in the 6 h chilling condition, e.g., fold difference of FPKM value (chilling Csa/Cmo leaf − chilling Csa/Csa leaf), was recorded as Δ2. (iii) The fold change in transcript abundance between chilling and control conditions, e.g., fold change of FPKM value (Δ2 − Δ1), was recorded as the Csa DEGs in the leaf. (iv) Genes with differences in transcript abundance with $\log_2$(fold change) >2 or $\log_2$(fold change) <−2 were identified as up- or downregulated DEGs, respectively.

The corresponding differential intense metabolites (DIMs), based on the ion intensity was analyzed as follows: (i) The difference in ion intensity values between the same tissues of heterografts and homografts in the control condition, i.e. the fold difference in ion intensity (control Csa/Cmo leaf − control Csa/Csa leaf), was recorded as the Δ1. (ii) The difference in ion intensity values between the same tissues in heterografts and homografts in the 6 h chilling condition, e.g., the fold change in ion intensity (chilling Csa/Cmo leaf − chilling Csa/Csa leaf), was recorded as the Δ2. (iii) The final difference between the values from chilling and control conditions, e.g., the fold change in ion intensity in (Δ2 − Δ1), was recorded as the multiple fold change of heterologous grafts in the chilling condition. (iv) The value of $\log_2$(Δ2 − Δ1) was used to verify DIM status: compounds with $\log_2$(Δ2 − Δ1) > 2 or $\log_2$(Δ2 − Δ1) <−2 were identified as up- or downregulated DIMs, respectively. Gene ID lists of DEGs and mobile mRNAs in different tissues of cucumber and pumpkin heterografts (Csa/Cmo, Cmo/Csa) and homografts (Csa/Csa, Cmo/Cmo) under both normal and chilling conditions were used for KEGG analysis.

Integrative analysis was performed as described by using Pearson correlation coefficient calculation for metabolome and transcriptome data integration. The mean of all biological replicates of each cultivar in the metabolome data and the mean value for the expression of each transcript in the transcriptome data were calculated. For example, the fold differences in Csa/Cmo leaves tissues were calculated from both the metabolome and transcriptome data and compared with those of the control Csa/Csa leaves under both control and 6 h chilling conditions. The coefficients were calculated from $\log_2$(fold change) of each metabolite and $\log_2$(fold change) of each transcript using Excel software. The relationship between metabolome, transcriptome and mobile mRNAs was performed based on KEGG map IDs using the Excel VLOOKUP function. We used Circos diagrams to analyze the correlation between the rootstock/scion of each heterologous grafting combination. Metabolome, transcriptome and mobile mRNA relationships were visualized using Cytoscape (version 3.8.1).

Determination of endogenous JAs and Isoleucine

The quantification of JAs was conducted at MetWare Biotechnology Co., Ltd. (Wuhan, China) using the AB Sciex QTRAP 6500 LC–MS/MS platform (https://sciex.com.cn/). Leaves from two-leaf-old transgenic cucumber and wild-type seedlings, weighing 50 mg, were harvested and frozen in liquid nitrogen. 1 μg/ml internal standards of JA (Jasmonic acid, Sigma, cat. no. J2500), JA-Ile (Jasmonoyl-L-isoleucine, OlChemim, cat. no. 0146233), MeJA (Jasmonic acid methyl ester, OlChemim, cat. no. 0412963) and OPDA (13-epi-12-Oxo-phytodienoic acid, OlChemim, cat. no. 0146193) were used. The calibration was performed as described in Pan et al.[55]. To enable quantification, 10 μL of an internal standard mixed solution (100 ng/mL) was added to the extract as internal standards (IS). They were then extracted by the solvent, 2-propanol/H_2O/ concentrated HCl (2:1:0.002, vol/vol/vol) strictly following the extraction protocol[55]. The samples were mixed with another 1 ml dichloromethane for 30 minutes at 4 °C, followed by centrifugation for 5 min at 13,000*g* and 4 °C. The solvent was transferred from the lower phase into a screw-cap vial and concentrated the solvent mixture (not completely dry) using a nitrogen evaporator with nitrogen flow. To avoid the loss of samples, Sep-Pak C18 solid-phase extraction (SPE) was not used in the extraction. The samples are redissolved in 0.1 mL of methanol. Fifty microlitres of the sample solution was injected into the reverse-phase C18 Gemini HPLC column. The triple quadrupole-linear ion trap mass spectrometer (QTRAP), QTRAP® 6500 + LC–MS/MS System, was equipped with an ESI Turbo Ion-Spray interface and operated in both positive and negative ion modes.

The ESI source operation parameters were as follows: ion source, ESI+/−; source temperature 550 °C; ion spray voltage (IS) 5500 V, Positive, −4500 V (Negative); curtain gas (CUR) was set at 35 psi, respectively. Phytohormones were analyzed using scheduled multiple reaction monitoring (MRM). The analysis was controlled by Analyst 1.6.3 software (Sciex)[56]. Multiquant 3.0.3 software (Sciex) was used to quantify all metabolites. Mass spectrometer parameters, including the delustering potentials (DP) and collision energies (CE) for individual MRM transitions, were optimized with further DP and CE optimization. Three biological replicates were performed, and each replicate included 4–6 individual cucumber plants.

For the measurement of isoleucine levels, the analysis was conducted at IGENECODE Co., Ltd. (Beijing, China). A UPLC system (ACQUITY UPLC; Waters, Milford, MA, USA) and a hybrid quadrupole time-of-flight (Q-TOF) tandem mass spectrometry (triple-TOF-MS/MS; Triple TOF 6545 system) were utilized following modifications[57]. Four biological replicates were performed, and each replicate included 4–6 individual cucumber plants. Statistical analysis was performed using IBM SPSS Statistics 27 v27.0.1. One-way ANOVA followed by Duncan's test was used ($p < 0.05$).

Virus-induced gene silencing (VIGS)

Specific sequences from the CDS of *CsaKARI* or *CsaJAR1* were cloned into the pTRSV(Tobacco RingSpot Virus) vector and transformed into *Agrobacterium* GV3101. Cucumber seedlings at the cotyledon stage were injected with a mixture of *Agrobacterium* containing pTRSV1 and pTRSV2 recombinant plasmids. The inoculated cucumber seedlings were placed in a growth chamber for cultivation. Cucumber Phytoene Desaturase (CsaPDS) construct (TRSV1: TRSV2-PDS, 1:1) used for silencing control. TRSV2 and TRSV1 empty vector (TRSV1: TRSV2-00,1:1) were used as a negative control. TRSV1:TRSV2-*CsaKARI* and TRSV1:TRSV2-*CsaJAR1* were used to inoculate cucumber wild type and CmoKARI1-TG transgenic cucumbers, respectively. When the plants grew to the two-leaf stage, the presence of TRSV1 and TRSV2 vectors in

the cucumbers was detected, and the silencing efficiency was verified using RT-qPCR. Plants with relatively high silencing efficiency (>70%) were selected for subsequent low-temperature treatment experiments.

DAB and NBT staining

DAB (3,3′-diaminobenzidine) and NBT (Nitrotetrazolium Blue chloride) staining were performed on the first true leaf of cucumber seedlings. DAB and NBT reagents were purchased from Beijing Coolaber Company. For DAB staining, 50 mg of DAB was added to a 50 ml centrifuge tube containing 45 ml of distilled water, followed by the addition of 25 µl Tween-20 and 2.5 ml of 200 mM Na_2HPO_4 to the tube to prepare a 10 mM Na_2HPO_4-DAB solution. Three true leaves from each of three seedlings were used as one biological replicate, and three biological replicates were performed for each treatment. For NBT staining, 0.1 g of NBT was dissolved in 50 ml of 50 mM phosphate buffer to prepare a 0.2% NBT staining solution. The intensity of DAB and NBT staining was analyzed by using ImageJ. Three true leaves from each of three seedlings were used as one biological replicate, and three biological replicates were performed for each treatment.

ELISA (enzyme-linked immunosorbent assay) for the determination of Ile and JA-Ile content

Ile and JA-Ile content in cucumber leaves were determined by using Plant ILE ELISA KIT (Shanghai Yiyan Biotechnology Co., Ltd., China) and Plant JA-Ile, Ile ELISA KIT (MyBioSource, SanDiego, USA; Shanghai Renjie) as described in the manual instructions. Cucumber leaves in different treatments were harvested from 5 to 6 individual plants randomly and combined into one replicate pool. At least three replicate pools were collected for each condition to analyze Ile and JA-Ile content. Each 0.15 g of ground sample mixed with PBS (pH 7.4) was centrifuged at 8000 rpm for 30 min at 4 °C, and the supernatant was used for Ile and JA-Ile content determination.

First, the standard curve was created according to the manual instructions. In summary, 50 µl of various concentrations of standard samples were added to 40 µl of diluted sample supernatant and 10 µl of sample solution. After adding 100 µl of conjugate reagent, the samples were then incubated at 37 °C for 60 min. Following the incubation, the liquid was discarded, and the wells were washed with washing solution five times. Subsequently, 50 µl each of Chromogen solution A and Chromogen solution B provided by the kit were added to each sample and incubated for 15 min at 37 °C in the dark. Finally, the reaction was halted by adding 50 µl of stop solution, and the optical density (OD) value was measured at a wavelength of 450 nm. The polynomial quadratic regression equation of the standard curve was then calculated using these two formulas:

Ile: C (content, pmol/L) = 459.23*(OD) − 73.249;

JA-Ile: C (content, pmol/L) = 171.09*(OD) + 20.545.

The formula to convert JA-Ile and Ile content in pmol/L into ng/g FW is as follows:

Ile or JA-Ile content (ng/g FW) = $C\,(\mathrm{pmol}/L) * M * 10\_ * V * X * 10^{-3}/W$

C signifies the solution concentration (pmol/L), M represents the molecular weight, V stands for the sample volume of 10 µl, X indicates the extraction factor of 70, and W denotes the sample weight of 0.15 g.

Fluorescein isothiocyanate (FITC)-labeled amino acids application in grafted seedlings

FITC-Isoleucine and FITC-leucine were synthesized by Xi'an Ruixi Biological Technology Co., Ltd. (http://www.xarxbio.com, Xi'an, China). Briefly, 4 g of FITC was dissolved in a solvent mixture of 50 mL N,N- Dimethylformamide (DMF) and water. L-Isoleucine, L-leucine (1.5 eq.) and disopropylethylamine (DIPEA) (3.0 eq.) were added until completely dissolved. The reaction was carried out at 25 °C for 0.5 h. The reaction mixture was concentrated under reduced pressure with a rotary vane vacuum pump (HR-21M, -30mmHg/1BAR (100 kpa)) at 50 °C for 20 min, and the crude product was eluted by dichloromethane: methanol = 10:1 at 25 °C for 2 h, and purified by silica gel chromatography column (200–300 mesh). The product was vacuum-dried at 25 °C for 2 days. The quality of synthesized FITC-Isoleucine and FITC-leucine was inspected by the detector (SPD-20A) and mass spectrometer (API3200) with chromatographic column (HPLC column Shim-pack GIST-HP C18, 3 µm, 150 mm × 2.1 mm), Liquid-mass conditions (Flow rate:0.2 ml/min, wavelength: 490 nm, Injection volume: 10 µl, Mobile phase: methanol, 20 mM ammonium acetate-ammonia buffer (pH 8.0), ESI+)

The roots of grafted cucumber/pumpkin and cucumber/cucumber seedlings were pretreated with 50 µM FITC-Isoleucine, or leucine solution for 12 h. The distilled water was used as the negative control[54]. Then, grafted seedlings were transferred to a climate chamber at low (4/4 °C) and normal (28/18 °C) temperature with a 14 h/10 h light/dark photoperiod and PPFD of 300 µmol m^{-2} s^{-1}. After 6 h of low temperature treatment, the distribution of FITC-Isoleucine and FITC-leucine in roots, stems, petioles and leaves of grafted seedlings was examined by confocal laser scanning microscope (TCSSP8, Lecia). FITC fluorescence signal was quantified by ImageJ software.

Statistical analysis

Statistical analysis was performed using IBM SPSS Statistics 27 v27.0.1. For time-series data where treatment is compared only with the control, one-way ANOVA followed by Dunnett's multiple comparisons test was used ($p < 0.05$). Conversely, in cases where pairwise comparisons are made between multiple data sets, one-way ANOVA followed by Duncan's test was used ($p < 0.05$).

Reporting summary

Further information on research design is available in the Nature Portfolio Reporting Summary linked to this article.

Data availability

All data supporting the results of this article are included within the article and its additional files. Source Data are provided with this paper. The original RNA sequencing data used in this study are deposited in the NCBI Small Read Archive under accession numbers PRJNA552914 and PRJNA673087. The accession code of all genes used in this study was obtained from the Cucurbit Genomics Database (Cucumber Gy14 v2 http://cucurbitgenomics.org/organism/16, *Cucurbita moschata* (Rifu) genome http://cucurbitgenomics.org/organism/9) or the NCBI and are provided in the Supplementary Dataset 8. Source data are provided with this paper.

References

1. Ding, Y., Shi, Y. & Yang, S. Advances and challenges in uncovering cold tolerance regulatory mechanisms in plants. *N. Phytol.* **222**, 1690–1704 (2019).
2. Zhu, J. K. Abiotic Stress Signaling and Responses in Plants. *Cell* **167**, 313–324 (2016).
3. Guan, W., Haseman, D. & Nowaskie, D. Rootstock evaluation for grafted cucumbers grown in high tunnels: yield and plant growth. *HortScience* **55**, 914–919 (2020).
4. Stockinger, E. J., Gilmour, S. J. & Thomashow, M. F. Arabidopsis thaliana CBF1 encodes an AP2 domain-containing transcriptional activator that binds to the C-repeat/DRE, a cis-acting DNA regulatory element that stimulates transcription in response to low temperature and water deficit. *Proc. Natl Acad. Sci. USA* **94**, 1035–1040 (1997).
5. Liu, Q. et al. Two transcription factors, DREB1 and DREB2, with an EREBP/AP2 DNA binding domain separate two cellular signal transduction pathways in drought- and low-temperature-responsive gene expression, respectively, in Arabidopsis. *Plant Cell* **10**, 1391–1406 (1998).

6. Warschefsky, E. J. et al. Rootstocks: diversity, domestication, and impacts on shoot phenotypes. *Trends Plant Sci.* **21**, 418–437 (2016).
7. Liu, W. et al. Transcriptomic and physiological analysis reveal that alpha-linolenic acid biosynthesis responds to early chilling tolerance in pumpkin rootstock varieties. *Front. Plant Sci.* **12**, 669565 (2021).
8. Guo, Y. et al. Abscisic acid mediates grafting-induced cold tolerance of watermelon via interaction with melatonin and methyl jasmonate. *Front. Plant Sci.* **12**, 785317 (2021).
9. Li, H. et al. Methyl jasmonate mediates melatonin-induced cold tolerance of grafted watermelon plants. *Hortic. Res.* **8**, 57 (2021).
10. Wang, L. et al. The essential role of jasmonate signaling in Solanum habrochaites rootstock-mediated cold tolerance in tomato grafts. *Hortic. Res.* **10**, uhac227 (2023).
11. Huang, H., Liu, B., Liu, L. & Song, S. Jasmonate action in plant growth and development. *J. Exp. Bot.* **68**, 1349–1359 (2017).
12. An, J. P., Wang, X. F., Zhang, X. W., You, C. X. & Hao, Y. J. Apple B-box protein BBX37 regulates jasmonic acid mediated cold tolerance through the JAZ-BBX37-ICE1-CBF pathway and undergoes MIEL1-mediated ubiquitination and degradation. *N. Phytol.* **229**, 2707–2729 (2021).
13. An, J. P. et al. Abscisic acid insensitive 4 interacts with ICE1 and JAZ proteins to regulate ABA signaling-mediated cold tolerance in apple. *J. Exp. Bot.* **73**, 980–997 (2022).
14. Qi, C. et al. Heat shock-induced cold acclimation in cucumber through CsHSFA1d-activated JA biosynthesis and signaling. *Plant J.* **111**, 85–102 (2022).
15. Chini, A. et al. The JAZ family of repressors is the missing link in jasmonate signalling. *Nature* **448**, 666–671 (2007).
16. Thines, B. et al. JAZ repressor proteins are targets of the SCF(COI1) complex during jasmonate signalling. *Nature* **448**, 661–665 (2007).
17. Xie, D. X., Feys, B. F., James, S., Nieto-Rostro, M. & Turner, J. G. COI1: an Arabidopsis gene required for jasmonate-regulated defense and fertility. *Science* **280**, 1091–1094 (1998).
18. Yan, J. et al. The Arabidopsis F-box protein CORONATINE INSENSITIVE1 is stabilized by SCFCOI1 and degraded via the 26S proteasome pathway. *Plant Cell* **25**, 486–498 (2013).
19. Schulze, A. et al. Wound-induced shoot-to-root relocation of ja-ile precursors coordinates arabidopsis growth. *Mol. Plant* **12**, 1383–1394 (2019).
20. Kehr, J. & Kragler, F. Long distance RNA movement. *N. Phytol.* **218**, 29–40 (2018).
21. Kondhare, K. R., Patil, N. S. & Banerjee, A. K. A historical overview of long-distance signalling in plants. *J. Exp. Bot.* **72**, 4218–4236 (2021).
22. Ruiz-Medrano, R., Xoconostle-Cazares, B. & Lucas, W. J. Phloem long-distance transport of CmNACP mRNA: implications for supracellular regulation in plants. *Development* **126**, 4405–4419 (1999).
23. Lucas, W. J. et al. Selective trafficking of KNOTTED1 homeodomain protein and its mRNA through plasmodesmata. *Science* **270**, 1980–1983 (1995).
24. Banerjee, A. K. et al. Dynamics of a mobile RNA of potato involved in a long-distance signaling pathway. *Plant Cell* **18**, 3443–3457 (2006).
25. Kim, M., Canio, W., Kessler, S. & Sinha, N. Developmental changes due to long-distance movement of a homeobox fusion transcript in tomato. *Science* **293**, 287–289 (2001).
26. Haywood, V., Yu, T. S., Huang, N. C. & Lucas, W. J. Phloem long-distance trafficking of gibberellic acid-insensitive RNA regulates leaf development. *Plant J.* **42**, 49–68 (2005).
27. Huang, N. C., Luo, K. R. & Yu, T. S. Mobility of antiflorigen and PEBP mRNAs in tomato-tobacco heterografts. *Plant Physiol.* **178**, 783–794 (2018).
28. Yang, L. et al. m(5)C Methylation guides systemic transport of messenger RNA over graft junctions in plants. *Curr. Biol.* **29**, 2465–2476 e2465 (2019).
29. Zhang, H. et al. Expression of tomato prosystemin gene in Arabidopsis reveals systemic translocation of its mRNA and confers necrotrophic fungal resistance. *N. Phytol.* **217**, 799–812 (2018).
30. Yang, L. et al. Noncell-autonomous HSC70.1 chaperone displays homeostatic feedback regulation by binding its own mRNA. *N. Phytol.* **237**, 2404–2421 (2023).
31. Duan, X. et al. PbWoxT1 mRNA from pear (Pyrus betulaefolia) undergoes long-distance transport assisted by a polypyrimidine tract binding protein. *N. Phytol.* **210**, 511–524 (2016).
32. Wang, S. et al. A chaperonin containing T-complex polypeptide-1 facilitates the formation of the PbWoxT1-PbPTB3 ribonucleoprotein complex for long-distance RNA trafficking in Pyrus betulaefolia. *N. Phytol.* **238**, 1115–1128 (2023).
33. Hao, L. et al. A constitutive and drought-responsive mRNA undergoes long-distance transport in pear (*Pyrus betulaefolia*) phloem. *Plant Sci.* **293**, 110419 (2020).
34. Devers, E. A. et al. Movement and differential consumption of short interfering RNA duplexes underlie mobile RNA interference. *Nat. Plants* **6**, 789–799 (2020).
35. Thieme, C. J. et al. Endogenous Arabidopsis messenger RNAs transported to distant tissues. *Nat. Plants* **1**, 15025 (2015).
36. Liu, W. et al. Rootstock-scion exchanging mRNAs participate in the pathways of amino acids and fatty acid metabolism in cucumber under early chilling stress. *Hortic. Res.* https://doi.org/10.1093/hr/uhac031 (2022).
37. Liu, W. et al. Identification of long-distance transmissible mRNA between scion and rootstock in cucurbit seedling heterografts. *Int. J. Mol. Sci.* https://doi.org/10.3390/ijms21155253 (2020).
38. Zhang, W. et al. tRNA-related sequences trigger systemic mRNA transport in plants. *Plant Cell* **28**, 1237–1249 (2016).
39. Wang, L., Sadeghnezhad, E. & Nick, P. Upstream of gene expression: what is the role of microtubules in cold signalling?. *J. Exp. Bot.* **71**, 36–48 (2020).
40. Li, Y. et al. Isoleucine enhances plant resistance against *Botrytis cinerea* via jasmonate signaling pathway. *Front Plant Sci.* **12**, 628328 (2021).
41. Staswick, P. E. & Tiryaki, I. The oxylipin signal jasmonic acid is activated by an enzyme that conjugates it to isoleucine in Arabidopsis. *Plant Cell* **16**, 2117–2127 (2004).
42. Van Moerkercke, A. et al. A MYC2/MYC3/MYC4-dependent transcription factor network regulates water spray-responsive gene expression and jasmonate levels. *Proc. Natl Acad. Sci. USA* **116**, 23345–23356 (2019).
43. Bao, H. et al. The developing xylem transcriptome and genome-wide analysis of alternative splicing in Populus trichocarpa (black cottonwood) populations. *BMC Genomics* **14**, 359 (2013).
44. Sureshkumar, S. et al. A genetic defect caused by a triplet repeat expansion in *Arabidopsis thaliana*. *Science* **323**, 1060–1063 (2009).
45. Tabib, A. et al. A polynucleotide repeat expansion causing temperature-sensitivity persists in wild irish accessions of *Arabidopsis thaliana*. *Front. Plant Sci.* **7**, 1311 (2016).
46. Heinemann, B. & Hildebrandt, T. M. The role of amino acid metabolism in signaling and metabolic adaptation to stress-induced energy deficiency in plants. *J. Exp. Bot.* **72**, 4634–4645 (2021).
47. Liu, Y. et al. Diverse nitrogen signals activate convergent ROP2-TOR signaling in Arabidopsis. *Dev. Cell* **56**, 1283–1295 e1285 (2021).
48. Cao, P. et al. Homeostasis of branched-chain amino acids is critical for the activity of TOR signaling in Arabidopsis. *Elife* https://doi.org/10.7554/eLife.50747 (2019).
49. Liu, Y. & Xiong, Y. Plant target of rapamycin signaling network: Complexes, conservations, and specificities. *J. Integr. Plant Biol.* **64**, 342–370 (2022).

50. Dong, Y. et al. TOR represses stress responses through global regulation of H3K27 trimethylation in plants. *J. Exp. Bot*. https://doi.org/10.1093/jxb/erac486 (2022).
51. Li, X. et al. m5C and m6A modifications regulate the mobility of pumpkin CHOLINE KINASE 1 mRNA under chilling stress. *Plant Physiol*. https://doi.org/10.1093/plphys/kiae511 (2024).
52. Dong, Y., Teleman, A., Jedmowski, C., Wirtz, M. & Hell, R. The Arabidopsis THADA homolog modulates TOR activity and cold acclimation. *Plant Biol. (Stuttg)* https://doi.org/10.1111/plb.12893 (2018).
53. Geng, S. et al. An efficient root transformation system for CRISPR/Cas9-based analyses of shoot-root communication in cucurbit crops. *Hortic. Res*. https://doi.org/10.1093/hr/uhab082 (2022).
54. Qin, Y. et al. γ-aminobutyric acid contributes to a novel long-distance signaling in figleaf gourd rootstock-induced cold tolerance of grafted cucumber seedlings. *Plant Physiol. Biochem*. **216**, 109168 (2024).
55. Pan, X., Welti, R. & Wang, X. Quantitative analysis of major plant hormones in crude plant extracts by high-performance liquid chromatography-mass spectrometry. *Nat. Protoc*. **5**, 986–992 (2010).
56. Flokova, K. et al. UHPLC-MS/MS based target profiling of stress-induced phytohormones. *Phytochemistry* **105**, 147–157 (2014).
57. Patti, G. J., Tautenhahn, R. & Siuzdak, G. Meta-analysis of untargeted metabolomic data from multiple profiling experiments. *Nat. Protoc*. **7**, 508–516 (2012).

Acknowledgements

We would like to thank Dr. Thierry Heitz (IBMP-CNRS, Strasbourg, France) and Prof. Dr. Xuna Wu (Yunnan University, Kunming, China) for their critical comments on our manuscript. We greatly thank the ikann-editorial team for their scientific editing. This work was supported by the National Natural Science Foundation of China (32372792) for W. Zhang, the 2115 Talent Development Program of China Agricultural University to W. Zhang, and the Earmarked Fund for China Agriculture Research System (CAS-23) to L. Gao.

Author contributions

Y. Dong, L. Gao, and W. Zhang conceived and designed the experiments; M. Zhang, W. Liu, C. Wang, S. Lin, Y. Lu, and X. Li performed the experiments; Y. Dong and W. Zhang wrote the paper; Y. Dong, W. Zhang, and X. Han revised the paper; M. Zhang, C. Xiang, W. Liu, Y. Chen, H. Cui, Y. Ma, and W. Zhang analyzed the data; All authors read the final version of this paper and approved it for publication.

Competing interests

The authors declare no competing interests.

Additional information

Supplementary information The online version contains supplementary material available at https://doi.org/10.1038/s41467-025-63228-1.

Correspondence and requests for materials should be addressed to Wenna Zhang.

Peer review information *Nature Communications* thanks Tien-Shin Yu and the other, anonymous, reviewer(s) for their contribution to the peer review of this work. A peer review file is available.